

Long term culture of genome-stable bipotent progenitor cells from adult human liver

Meritzell Huch^{*,1,6,#}, Helmuth Gehart^{1#}, Ruben van Boxtel^{1,#}, Karien Hamer¹, Francis Blokzijl¹, Monique MA Versteegen², Ewa Ellis⁵, Martien van Wenum³, Sabine A Fuchs⁴, Joep de Ligt¹, Marc van de Wetering¹, Nobuo Sasaki¹, Susanne J. Boers⁴, Hans Kemperman⁴, Jeroen de Jonge², Jan NM Ijzermans², Edward Niewenhuis⁴, Ruurdje Hoekstra³, Stephen Strom⁵, Robert RG Vries¹, Luc JW van der Laan², Edwin Cuppen¹, Hans Clevers^{*,1}

¹Hubrecht Institute–KNAW and University Medical Centre Utrecht, Uppsalalaan 8, 3584CT, Utrecht, The Netherlands

²Erasmus MC-University Medical Center, Dept. of Surgery, Wytemaweg 80, 3015 CN

³Surgical laboratory and Tytgat Institute for Liver and Intestinal Research, Academic Medical Center, Meibergdreef 9, 1105 AZ Amsterdam, The Netherlands.

⁴University Medical Centre Utrecht

⁵Division of Pathology, Department of Laboratory Medicine, Karolinska Institute, Karolinska University Hospital Huddinge, Stockholm, Sweden

⁶ Present address: Wellcome Trust/ Cancer Research UK Gurdon Institute, Department of Physiology, Developmental Biology and Neurosciences, University of Cambridge. Tennis court Road, CB2 1QN, Cambridge UK.

#these authors contributed equally

*Correspondence: h.clevers@hubrecht.eu; m.huch@gurdon.cam.ac.uk

Summary

Despite the enormous replication potential of the human liver, there are currently no culture systems available that sustain hepatocyte replication and/or function *in vitro*. We have shown previously that single mouse Lgr5+ liver stem cells can be expanded as epithelial organoids *in vitro* and can be differentiated into functional hepatocytes *in vitro* and *in vivo*. We now describe conditions allowing long-term expansion of adult bile duct-derived bi-potent progenitor cells from human liver. The expanded cells are highly stable at the chromosome and structural level, while single base changes occur at very low rates. The cells can readily be converted into functional hepatocytes *in vitro* and upon transplantation *in vivo*. Organoids from α 1-antitrypsin deficiency and Alagille Syndrome patients mirror the *in vivo* pathology. Clonal long-term expansion of primary adult liver stem cells opens up experimental avenues for disease modeling, toxicology studies, regenerative medicine and gene therapy.

Highlights

- Establishment of a long-term human liver organoid culture
- Human liver stem cells retain genetic stability after long-term expansion
- Liver organoid cultures differentiate to functional hepatocytes *in vitro* and *in vivo*
- Organoids derived from patients with genetic disorders model liver disease *in vitro*

Introduction

The liver is the largest organ in the human body, and is mainly composed of two different epithelial cell types, hepatocytes and ductal cells. It synthesizes essential serum proteins and plays a key role in the homeostasis of metabolism and in the detoxification of a wide variety of endogenous and exogenous molecules. All these functions are performed primarily by hepatocytes (Duncan et al., 2009). Despite the considerable replication capacity of hepatocytes *in vivo* (Michalopoulos, 2013), liver cells have essentially resisted long-term expansion in culture (Casciano, 2000; Mitaka, 1998). Indeed, a recent study describes a human liver hepatocyte culture system with preservation of hepatocyte function, yet overall expansion cell numbers was 10-fold and the culture could only be expanded over a period of ~ 1 week (Shan et al., 2013).

Stem cells (ES, iPS or adult tissue-resident stem cells) represent an attractive alternative cell source, because of their unlimited self-renew capacity. Both, hES and hiPS cells have been differentiated towards hepatocyte-like cells in a stepwise manner using defined factors. However, recent reports have unveiled that genetic and epigenetic aberrations occur during the derivation and reprogramming process (Liang and Zhang, 2013; Pera, 2011). These range from chromosomal abnormalities (Laurent et al., 2011), sub-chromosomal changes such as “*de novo*” copy number variations (CNVs) (Hussein et al., 2011) and point mutations in protein coding regions (Gore et al., 2011). Such changes may complicate their use for regenerative medicine purposes (Bayart and Cohen-Haguener, 2013).

We have recently described a novel culture system that allows the long-term expansion (>1 year) of single mouse adult intestine (Sato et al., 2009), stomach (Barker et al., 2010), liver (Huch et al., 2013b) and pancreas (Huch et al., 2013a) stem cells. *Lgr5*, the receptor for the Wnt agonists R-spondins (Carmon et al., 2011; de Lau et al., 2011), marks adult stem cells in these mouse tissues (Barker et al., 2010; Barker et al., 2007; Huch et al., 2013a; Huch et al., 2013b). Furthermore, these cultures remain committed to their tissue-of-origin, that is, intestinal stem cells only generate organoids harboring intestinal lineages. We have recently adapted the technology to allow culturing of human intestinal stem cells (Jung et al., 2011; Sato et al., 2011), and shown that patient-derived intestinal organoids recapitulate the pathology of hereditary intestinal diseases (Bigorgne et al., 2014; Dekkers et al., 2013; Wiegerinck et al., 2014). Here, we pursue the establishment of an organoid culture system for human liver.

Results

Optimization of human liver stem cell culture

We recently described a defined mouse liver culture medium that allows long-term expansion of mouse liver stem cells in culture in the absence of a mesenchymal niche (Huch et al., 2013b). This cocktail (ERFHNic, or ‘mouse liver medium’) supported the growth of human liver cells only for 2-3 weeks, after which the cultures quickly deteriorated (Figure 1A-B and Figure S1A, top panel). We then sought to define a culture system that would allow the long-term expansion of human liver cells *in vitro*. Gene expression profiles of human liver cultures that were maintained for 2 weeks in ‘mouse liver medium’ revealed that the Tgf- β signaling pathway was highly activated in the cultures. Tgf- β target genes such as *CTGF*, *PLAT*, *TIMP1* and *TIMP2* (Dooley and ten Dijke, 2012; Verrecchia et al., 2001) were highly

expressed while Tgf- β sequesters (*LTBP2* and *LTBP3*) and Smad4 inhibitors (*SMURF1* and *SMURF2*) (Massague et al., 2005) were virtually absent (Figure S1B). It is known that Tgf- β signaling results in growth arrest (Massague et al., 2000) and epithelial-to-mesenchymal transition *in vivo* (Xu et al., 2009). Specific inhibition of Tgf- β receptors Alk4/5/7 by the small molecule inhibitor A8301, which does not target the BMP-GDF Alk receptors (Alk1/2/3/6) (Schmierer and Hill, 2007), resulted in downregulation of the Tgf- β target genes *CTGF*, *TIMP2*, *PLAT* (Figure S1C) and in a significant increase in colony forming efficiency (Figure 1D). More importantly, upon A8301 addition, the cells expanded for longer period of time in culture (~6-7 weeks, 6-7 splits) (Figure 1B). However, after that period, the cultures again deteriorated (Figure 1B and Figure 1C, left panel). We noticed that the expression of the progenitor/stem cell marker *LGR5* decreased over time, while differentiation markers such as Albumin (*ALB*) or *CYP3A4* were upregulated (not shown), indicating that our conditions were promoting differentiation at the cost of self-renewal and long-term maintenance of liver progenitor cells in culture.

In addition to A8301, we then tested candidate compounds to induce liver cell proliferation and/or Lgr5 expression in culture (see Table S1). Liver progenitors have been identified in the ductal tree, both during homeostasis (Furuyama et al., 2011) and after damage (Dorrell et al., 2011; Huch et al., 2013b; Shin et al., 2011). Mouse liver organoids containing Lgr5+ cells are largely composed of bile duct-derived bi-potent progenitor/stem cells. Similarly, human liver organoid cultures maintained in mouse medium supplemented with TGF inhibitor were mainly composed of ductal-like cells. Because administration of Forskolin (FSK), a cAMP pathway agonist, results in enhanced proliferation of biliary duct cells *in vivo* (Francis et al., 2004), we asked whether cAMP would support the human liver cultures.

In the presence of FSK, *LGR5* and the ductal marker *KRT19* were upregulated, while the expression of the hepatocyte differentiation markers *ALB* and *CYP3A4* decreased (Figure S1D). Colony forming efficiency was essentially unchanged, when compared to A8301 treatment alone (Figure 1D), but upon FSK treatment, the cultures expanded for many months in culture (> 6 months) maintaining a weekly split ratio of 1:4-1:6 (Figure 1B). The cells grew out into organoids that formed budding domains also observed in mouse liver cultures (Figure 1C, right panel). Similar results were observed when other cAMP agonists were used (8-BrcAMP, Cholera toxin or NKH477) (Figure S1E). Consistent with this, removal of cAMP agonists (e.g. FSK) resulted in rapid loss of proliferation and deterioration of the cultures (Figure S1F-G). Similarly, removal of the Wnt agonist R-spo or blockage of Wnt secretion by porcupine inhibition (IWP-2) resulted in rapid deterioration and loss of the cultures (Figure S1F-H). This effect was rescued by exogenous addition of Wnt in the medium (Figure S1H), again indicating that active Wnt signaling is essential for the long-term expansion of the cultures.

To generalize our findings across multiple donors, we obtained 12 additional healthy human donor liver biopsies and cultured them in our improved human liver medium. Table S2 summarizes the data. Under our improved conditions (ERFHNic + Tgfbi + FSK), all 12 human liver-derived cultures grew exponentially, with a consistent doubling time of ~60h independent of the age of the culture (2 weeks or 3 months) (Figure 1E/F). EdU incorporation confirmed that the cells maintained their proliferative state *in vitro* (Figure 1G) 3 months after the initiation of culture. Of note, cultures grown under these culture conditions could be readily frozen and thawed (data not shown). Overall, these results indicated that the

combination of Wnt signaling and cAMP activation, combined with Tgf- β inhibition, is essential to sustain long-term expansion of human liver progenitors *in vitro*.

Human liver organoid cultures initiate from ductal cells

To assess the cell-of-origin of our cultures, we FACS-purified hepatocytes and duct cells from 3 independent human hepatocyte isolations instead of liver biopsies. Hepatocyte isolations by collagenase perfusion yield high numbers of fresh, viable and functional human hepatocytes that are used for hepatocyte transplantation infusions (Gramignoli et al., 2012) (Figure S2A). We employed EpCAM to differentially sort hepatocytes (EpCAM⁻) from ductal cells (EpCAM⁺, bile duct and canal of herring ductal /progenitor cells, Figure 1H and Figure S2B and S2C) (Schmelzer et al., 2007; Yoon et al., 2011). While hepatocytes did not yield organoids in our cell culture conditions (colony formation efficiency 0%), ductal (EpCAM⁺) cells developed into long-term, self-renewing organoid structures with a striking efficiency of $28.4 \pm 3.2\%$ (Figure 1H and Figure S2D-E). When crude hepatocyte preparations (not differentially sorted) were directly cultured, cells grew into organoid structures with an efficiency that correlated directly with the amount of residual EpCAM⁺ cells in the crude preparation (Figure S2F-G). Therefore, we concluded that in our culture system ductal cells and not hepatocytes revert to a bi-potential progenitor state.

Human liver cultures established from single human liver cells are genetically stable

Genetic stability is a concern for the future application of cells that have undergone derivation and expansion in culture (Lund et al., 2012). Adult stem cells may have evolved to minimize the risk of accumulating somatic mutations (Cairns, 1975). Indeed, karyotyping of clonal human liver organoids cultured for 3 months revealed that the cells maintain normal chromosome numbers over time (Figure 3A and Figure S4A). The ability to repeatedly generate clonal cultures from single liver stem cells allowed us to isolate sufficient DNA for WGS analysis and subsequent characterization of the mutational load present in the cultured cells after several months of *in vitro* expansion (Figure 2A).

From two donors, we obtained biopsy samples, which we dissociated and cultured in bulk for 7 days. Subsequently, we isolated single cells by flow cytometry and established 2 independent clonal lines for each of the two livers (cultures A and B). After 3 months of expanding these cultures, a second cloning step was performed. The combined procedure allowed us to determine all the genomic variation that had accumulated in a single cell during life, derivation, and 3 months of culturing (Figure 2B).

We observed 720 – 1424 base substitutions per cultures of which only a small part was introduced during the 3 months culture, which is equivalent to 13 weekly passages (63 – 139; Figure 2C). The majority of the base substitutions were therefore incorporated during life or introduced during organoid derivation. Interestingly, we observe twice as many base substitutions in both cultures derived from donor 1 compared to the cultures derived from donor 2 (Figure 2C). This is most probably the result of the high age of donor 1 (74 years) compared to donor 2 (30 years), suggesting that the majority of the somatic base substitutions we observed were acquired during life.

How do these numbers compare to published data? It has been reported that iPS cells contain 1,058 – 1,808 *de novo* base substitutions per line (determined at passage numbers between 15 and 25) when compared to their parental somatic cells (Cheng et al., 2012). Of note, these numbers do not include the variation acquired *in vivo* in the parental somatic cells, which we did determine here for the clonal liver organoid cultures. We therefore conclude that liver

organoid cultures accumulate in the order of 10-fold fewer base substitutions during *in vitro* expansion compared to iPS cells. Of the total number of base substitutions only few were located in protein coding DNA (7 – 9 base substitutions per culture; Figure 2D). With the exception of one synonymous mutation in culture A from donor 2 (Table S3), all mutations were already present in the early passage clonal cultures, indicating that they were incorporated during life or organoid derivation and not during 3 months-expansion. None of the mutated genes occurs in COSMIC databases (Table S3). In iPS cells, it has been reported that an average of 6 base substitutions per line affect protein coding DNA (Cheng et al., 2012; Gore et al., 2011) which were reported to be enriched for genes mutated or being drivers in cancers (Gore et al., 2011).

Next, we checked for evidence of chromosomal aberrations in the WGS data of the different liver organoid cultures. In line with our karyotyping analysis, we did not observe any chromosomal aberration (Figure 3B). We observed 2 copy number variants (CNVs), heterozygous gains, in one of the liver organoid cultures (Figures 3C). In the other cultures, we did not detect any CNV (Figure 3D and Figure S4). Moreover, these 2 CNVs were already present in the early passage cultures and therefore did not result from long-term culturing, suggesting they were either acquired *in vivo* or during organoid derivation. ES cell cultures routinely show abnormal karyotypes (Baker et al., 2007) and iPS cells have been reported to harbor considerable amounts of somatic CNVs (Hussein et al., 2011; Laurent et al., 2011) (Martins-Taylor et al., 2011; Mayshar et al., 2010) (Abyzov et al., 2012), complicating their clinical use.

Human liver cultures express markers of ductal and hepatocyte lineages

We next examined the lineage potential of our liver stem cell cultures. The stem cell markers *PROM1* and *LGR5*, as well as ductal (*SOX9*, *OC2*) and hepatocyte markers (*HNF4a*) were readily expressed (Figure 4A and Figure S5A-B). Histologically, liver organoids displayed a duct-like phenotype characterized by two types of epithelia: 1) a single-layered epithelium formed by polarized cells with basal nuclei, expressing cytokeratin epithelial markers (*KRT19* and *KRT7*), and 2) a pseudo-stratified epithelium with non-polarized E-Cadherin⁺ HNF4a⁺ and some KRT7⁺ cells (Figure 4B-D). *SOX9* (Figure 4E) and *EPHB2* (Figure 4F) were detectable in almost all the cells within an organoid while *LGR5* was detectable within the *EPHB2*⁺ population (Figure 4F).

Differentiation into functional hepatocytes *in vitro* and upon transplantation

Similar to what we had observed with the mouse liver organoid cultures under expansion conditions, the human counterparts failed to express markers of mature hepatocytes, such as Albumin or CYP3A4 (Figure 4A and Figure 5C, EM bars). Therefore, we defined a human differentiation medium (DM) by combining our acquired knowledge on mouse hepatocyte differentiation with known hepatocyte differentiation-promoting compounds (Table S1). Removal of the growth stimuli R-spo and FSK directly resulted in the up-regulation of Albumin and CYP3A4 gene expression (Figure S5C). To this medium, we then added the Notch inhibitor DAPT (Huch et al., 2013b), FGF19 (Wu et al., 2011) and dexamethasone (Rashid et al., 2010) (Figure S5D). BMP7 is known to accelerate liver regeneration and hepatocyte proliferation *in vivo* (Sugimoto et al., 2007). When testing compounds to improve our culture conditions, we noticed that BMP7 slightly facilitated the expression of hepatocyte markers ALB and CYP3A4, without compromising the proliferation ability of the culture itself (data not shown). Therefore, 5-7 days prior to the start of differentiation, we supplemented the expansion medium (EM) with 25ng/ml BMP7, which was then maintained

during the differentiation step (Figure 5A). Using this combination of growth factors (BMP7, FGF19, HGF and EGF), small molecule inhibitors (DAPT and A8301) and Dexamethasone, the cells acquired pronounced hepatocyte morphologies, including polygonal cell shapes, as made visible by ZO-1 staining (Figure 5B). We subsequently examined the level of maturity of the differentiated cells by using gene expression profiling, immunofluorescence and various biochemical assays.

Gene expression profiles proved that the differentiated cultures expressed high levels of hepatocyte markers (Figure 5D). Hepatocyte specific genes such as ALB, several cytochrome enzymes, Apolipoproteins (APOB) and several complement factors (C3) were readily expressed upon differentiation in all 4 donors analyzed (Figure 5D). We confirmed these results by qPCR and RT-PCR analysis for selected genes (ALB, several cytochromes, and TAT) (Figure 5C and Figure S5E) and found that the differentiated cultures express levels of cytochrome CYP3A4 expression similar to that of human liver tissue. A 100-1000x fold increase in Albumin expression was also detected on the DM-treated cultures, although the expression levels were still 1000x lower when compared to freshly isolated human liver material. Immunofluorescence visualized cells with high levels of ALB and MRP4 within the organoids (Figure 5B). Similar results were obtained with cultures derived from EpCAM⁺ sorted cells (Figure S5F-G)

We next assessed the ability of the hepatocyte cells to retain hepatocyte function *in vitro*. Immunohistochemistry analysis indicated that the cells could accumulate glycogen (Figure 6A) and take up LDL (Figure 6B). Biochemical analyses demonstrated that the differentiated cells secreted high levels of Albumin into the medium (Figure 6C). Cytochrome family members, such as Cyp3a4, are expressed exclusively in mature hepatocytes. They play an important detoxifying function for exogenous molecules in the liver (Casciano, 2000). Upon differentiation, the cultures exhibited similar p450-3A4 activity as fresh isolated hepatocytes (Figure 6D, compare to Figure S2A). We also observed that the differentiated cultures hydroxylated midazolam, another indication of functional CYP3A3/4/5 activity (Wandel et al., 1994), and glucuronidated hydroxy-midazolam, thereby showing evidence of both phase I and II detoxifying reactions (Figure 6E). We then assessed the ability of the cultured cells to synthesize bile acids, a hallmark of hepatocyte function. Upon differentiation, bile acid salts were readily secreted into the medium (Figure 6F). Finally, the cultures also exhibited the ability to detoxify ammonia at similar levels to HepaRG cells (Figure 6G). In all cases, the expanded human liver organoids showed stronger hepatocyte functions when compared to the standard/reference cell line HepG2 cells (Figure 6).

To test the ability of the cultures to engraft in damaged tissue and to fully differentiate into functional hepatocytes *in vivo*, we treated Balb/c nude mice with CCl₄-retorsine to induce acute liver damage. As shown by others, this treatment is permissive for the engraftment of hepatocytes (Guo et al., 2002; Schmelzer et al., 2007). Using human-specific antibodies (Figure S6A), we initially detected Krt19 positive, ductal-like cells at 2h and d2 after transplantation, distributed throughout the liver parenchyma (Figure S6B). At later time points, we observe Albumin⁺, Krt19⁻ human cells as singlets or doublets or, more rarely, in larger hepatocyte foci in the mouse liver (Figure 6H and Figure S6C). This agreed with the non-chronic nature of our damage model, which provides no stimulus for expansion of the transplant after the initial engraftment. We detected human Albumin and human alpha-1-antitrypsin in the circulation of recipient mice within 7-14 days (Figure 6I and Suppl Figure 6D/E), at a level that remained stable for more than 60 days in 5/6 mice and for more than

120 days in 2/5 animals. While transplantation of primary human hepatocytes initially yielded higher levels of human Albumin in mouse circulation (Figure 6I), the levels approximated those of transplanted organoids within a month. Presence of human albumin and human alpha-1-antitrypsin in mouse serum proved, together with Albumin and Krt19 stainings, that transplanted cells differentiated into human hepatocytes *in vivo*.

Organoids from human patients model disease pathogenesis *in vitro*

Encouraged by the establishment of a culture medium that allows the long-term expansion of genetically stable liver cells, we explored whether our culture system would be suitable for disease modeling. A1AT deficiency is an inherited disorder that predisposes to chronic obstructive pulmonary disease and chronic liver disease (Stoller and Aboussouan, 2005). Alpha-1 antitrypsin is a protease produced in the liver, which functions to protect the lung against proteolytic damage from neutrophil elastase. The most frequent mutation causing a severe phenotype is the Z allele, which involves a substitution of glutamic acid with lysine at position 342 (Glu342Lys) in the SERPINA1 gene, which causes accumulation of misfolded α 1-antitrypsin in the endoplasmic reticulum of hepatocytes. The ZZ mutant phenotype is characterized by a ~80% reduction of the protein in plasma, which subsequently causes lung emphysema (Stoller and Aboussouan, 2005).

We obtained human liver biopsies from 3 patients diagnosed with A1AT deficiency who were undergoing liver transplantation (Table S2). Biopsies were divided into samples for histological characterization, RNA isolation, DNA isolation and for expansion in culture. We confirmed that all 3 patients carried the homozygous Z allele (PiZZ), by Sanger sequencing of the SERPINA1 locus (Figure S7A). The isolated cells rapidly grew into 3-D structures generating organoids that closely resembled the organoids derived from healthy biopsies (Figure 7A) and were grown for >4 months in culture at a 1:5 split ratio/week, similar as the cultures derived from healthy/donor biopsies.

We then confirmed the ability of the A1AT-D derived cultures (PiZZ cultures) to differentiate into functional hepatocytes *in vitro*. Gene expression analysis demonstrated that the cells differentiated normally. When submitted to hierarchical clustering analysis, differentiated organoids derived from A1AT-deficient patients clustered together with differentiated organoids derived from healthy donor biopsies (Figure S7B). Of note, functional tests revealed that the differentiated cells from A1AT patients secrete high levels of Albumin and take up LDL similar to healthy donor-derived organoid cultures (Figure 7B-D).

We then analyzed the ability of the cultured cells to mimic the pathology of the disease *in vitro*. Functional, healthy hepatocytes secrete A1AT protein into the bloodstream to inhibit neutrophil elastase mainly in the lungs (Figure 7E). In A1AT-deficiency, the molecular pathogenesis of the liver disease relates to the aggregation of the protein within the endoplasmic reticulum of hepatocytes (Lawless et al., 2008). A1AT-Protein aggregates were readily observed within the cells of the differentiated organoids derived from the A1AT-D patient (Figure 7H), similar to what was found in the original biopsy (Figure 7G), while these aggregates were essentially absent from the organoids derived from healthy donor-material (Figure 7F). A1AT ELISA confirmed reduced secretion of the protease inhibitor from PiZZ organoids (Figure 7I), which mimics the reduced A1AT serum levels in patients (Table S2 indicates the A1AT secretion per patient). Likewise, supernatants from differentiated ZZ mutant organoids showed a strongly reduced ability to block elastase activity (Figure 7J).

Advanced stages of A1AT deficiency are characterized by liver injury and cirrhosis due to combined effects of uncontrolled protease activity and apoptotic loss of functional hepatocytes (Fairbanks and Tavill, 2008). Protein misfolding and resulting ER Stress are the primary causes that drive hepatocytes from PiZZ individuals to eventual apoptosis (Lawless et al., 2008). Differentiated liver organoids from A1AT-D patients mimicked the *in vivo* situation and showed signs of ER stress, such as phosphorylation of eIF2 α (Figure 7K) and a slight increase in apoptosis in the differentiated state (Figure S7C and D).

Using a biopsy from a patient suffering from Alagille syndrome (AGS), we tested whether structural defects of the biliary tree can also be modeled. AGS is a rare genetic disorder caused by mutations in the Notch signaling pathway, which results in partial to complete biliary atresia (Kamath et al., 2013). Patient organoids could be expanded at normal rates and showed no obvious difference to donor in the undifferentiated state. However, upon differentiation to the biliary fate by withdrawal of R-spondin, Nicotinamide, TGF β i and FSK from the culture medium, AGS patient organoids failed to upregulate biliary markers such as *KRT19* and *KRT7*, while donor (wildtype, wt) organoids readily did (Figure S7E). Staining for KRT19 revealed that biliary cells were reduced in numbers and were unable to integrate into the epithelium. Rather, they rounded up and underwent apoptosis inside the organoid (Figure S7F). This finding is in line with AGS mouse models, which show that *Jagged-1/Notch2* is dispensable for biliary lineage specification, but required for biliary morphogenesis (Geisler et al., 2008; McCright et al., 2002). Thus, AGS liver organoids mimic the patient phenotype and constitute the first human 3D model system to study Alagille syndrome.

Discussion

Liver diseases range from genetic inherited disorders (e.g. Alpha-1 antitrypsin or Alagille Syndrome) to viral hepatitis, liver cancer and obesity-related fatty liver disease. Overall, these account for the eighth-related cause of death in the United States (Asrani et al., 2013). Failure in the management of liver diseases can be attributed as much to the shortage of good quality donor livers (Vilarinho and Lifton, 2012) as to our poor understanding of the mechanisms behind liver pathology. The latter is mainly due to the lack of good *in vitro* models that allow the expansion of functional human liver cells that faithfully recapitulate the pathology of the associated disease.

The value of any cultured cell as disease model or as a source for cell therapy transplantation depends as much as on the fidelity and robustness of its expansion potential as well as on its ability to maintain a normal genetic and epigenetic status (Pera, 2011). The possibility of differentiating hESC or reprogrammed fibroblasts (iPS) into almost any differentiated cell type, from neurons to hepatocytes, has allowed modeling of many human genetic diseases including A1AT-D (Rashid et al., 2010). However, the genetic instability of the cultured stem cells (as outlined in the Introductory section) raises concerns regarding their safe use in cell therapy transplantation (Bayart and Cohen-Haguenaer, 2013).

Here, we show that primary human liver cells obtained from a donor liver can readily be expanded *in vitro* into 3D organoid cultures. These cells self-renew and differentiate into functional hepatocyte cells *in vitro* and generate bona-fide hepatocytes *in vivo*, upon

transplantation. Our extensive analysis of the genetic stability of cultured organoids *in vitro* demonstrates that the expanded cells preserve their genetic integrity after months in culture.

Under our culture conditions, only ductal (but not hepatocyte) cells, acquire a bi-potent progenitor state and can differentiate into the two epithelial lineages of the liver: ductal and hepatocyte. These results agree with our previous observations in the mouse (Huch et al., 2013b), yet are in striking contrast to recent publications where, utilizing several lineage tracing approaches, ductal/resident stem cells were shown little contribution to mouse liver regeneration (Schaub et al., 2014; Yanger et al., 2014; Yanger et al., 2013). While our experiments do not address the extent to which this ductal population contributes to physiological hepatocyte regeneration in humans, our results resemble what has been elegantly shown in zebrafish and rat models: in the event of an almost complete hepatocyte loss or blockage of hepatocyte proliferation, biliary epithelial cells convert into hepatocytes to regenerate zebrafish (Choi et al., 2014) and rat livers (Michalopoulos, 2014). Our data is further corroborated by recent observations made in human fulminant hepatic failure, where huge numbers of proliferating EpCAM+ biliary epithelial cells are observed (Hattoum et al., 2013). These might be responsible for the rapid spontaneous recovery observed in some of these patients (up to 30%), by contributing to the generation of the *de novo* repaired hepatocyte pool (Michalopoulos, 2014).

Furthermore, as a proof-of-concept, we show that the cells from patients suffering from an inherited metabolic liver disease, such as A1AT-deficiency, can be expanded *in vitro* and partially reproduce the features present on the A1AT-deficiency pathology. Translating such a system to the study of other inherited liver diseases, which often lack good *in vitro* and *in vivo* models, has the potential to increase our knowledge on the molecular pathogenesis of these, often abandoned, liver disorders. Indeed, we demonstrate that organoids derived from an Alagille Syndrome patient, a rare disorder affecting the architecture of the liver biliary tree, can be readily expanded and reproduce the structural duct defects present in the livers of these patients. Repair by homologous recombination using CRISPR/Cas9 technology is feasible in organoid cultures, as we have recently demonstrated in colon stem cells of Cystic Fibrosis patients (Schwank et al., 2013). A variety of monogenic hereditary diseases affect the liver specifically, and these should all be amenable to a comparable *in vitro* approach of gene repair in clonal liver stem cells, thus opening up the avenue to design personalized treatments for these patients. Overall, our results open up the avenue to start testing human liver material expanded *in vitro* as an alternative cell source for studies of human liver regeneration, human liver disease mechanism, cell therapy transplantation, toxicology studies or drug testing.

Experimental Procedures

Human liver organoid culture

Liver biopsies (0.5-1cm³) were obtained from donor and explant livers during liver transplantation performed at the Erasmus MC, Rotterdam. The Medical Ethical Council of the Erasmus Medical Center approved the use of this material for research purposes and informed consent was provided by all patients. Liver cells were isolated from human liver biopsies (0.5-1cm³) by collagenase-accutase digestion as described in Supplemental Experimental Procedures. The different fractions (collagenase and accutase) were mixed and washed with

cold Advanced DMEM/F12 and spun at 300-400g for 5 min. The cell pellet was mixed with Matrigel (BD Biosciences) or Reduced Growth Factor BME 2 (Basement Membrane Extract, Type 2, Pathclear) and 3000-10000 cells were seeded per well in a 48well/plate. Non-attaching plates were used (Greiner). After Matrigel or BME had solidified, culture medium was added. Culture media was based on AdDMEM/F12 (Invitrogen) supplemented with 1%N2 and 1%B27 without retinoic acid (both from Gibco), 1.25 mM N-Acetylcysteine (Sigma), 10 nM gastrin (Sigma) and the growth factors: 50 ng/ml EGF (Peprotech), 10% RSPO1 conditioned media (home-made), 100 ng/ml FGF10 (Peprotech), 25ng/ml HGF, 10mM Nicotinamide (Sigma), 5uM A83.01 (Tocris) and 10uM FSK (Tocris). For the establishment of the culture, the first 3 days after isolation the medium was supplemented with 25ng/ml Noggin (Peprotech), 30% Wnt CM (home-made prepared as described in (Barker et al., 2010) and 10 uM (Y27632, Sigma Aldrich) or hES Cell cloning Recovery solution (Stemgent). Then, the medium was changed into a medium without Noggin, Wnt, Y27632, hES Cell cloning Recovery, solution while 25ng/ml BMP7 (Peprotech) were supplemented on top. The latter addition is optional. After 10-14 days organoids were removed from the Matrigel or BME, mechanically dissociated into small fragments, and transferred to fresh matrix. Passage was performed in 1:4-1:8 split ratio once every 7-10 days for at least 6 months. To prepare frozen stocks, organoid cultures were dissociated and mixed with Recovery cell culture freezing medium (Gibco) and froze following standard procedures. When required, the cultures were thawed using standard thawing procedures and cultured as described above. For the first 3 days after thawing, the culture medium was supplemented with Y-27632 (10 μ M).

Growth curves and expansion ratios were performed and calculated as described in Supplemental Experimental Procedures.

Isolation of EpCAM+ cells and single cell (clonal) culture

Cell suspensions prepared as described in Supplemental Experimental Procedures were stained with Anti-Human CD326 (EpCAM), sorted on a MoFlo (Dako Cytomation) sorter and cultured as described above with medium supplemented with Y-27632 (10 μ M, Sigma Aldrich) for the first 4 days. Passage was performed in split ratios of 1:4-1:8 once per week. For clonogenic assays, single cell suspensions were sorted using FSC and pulse width to discriminate single cells. Propidium iodide staining was used to label dead cells and FSC: Pulse-width gating to exclude cell doublets (MoFlow, Dako). Sorted cells were embedded in Matrigel and seeded in 96 well plates at a ratio of 1 cell/well. Cells were cultured as described above.

Hepatocyte differentiation and *in vitro* functional studies

Liver organoids were seeded and kept 7-10 days under the liver expansion conditions explained above supplemented with BMP7 (25ng/ml). Then, the cultures were split and seeded accordingly in this expansion medium supplemented with BMP7 for at least 2-4 days. Then, medium was changed to the differentiation medium (DM): AdDMEM/F12 medium supplemented with 1%N2 and 1% B27 without retinoic acid (both from Gibco) and containing EGF (50 ng/ml), gastrin (10nM, Sigma), HGF (25ng/ml, Peprotech), FGF19 (100 ng/ml), A8301 (500 nM, Tocris Bioscience), DAPT (10 uM, Sigma), BMP7 (25ng/ml) and Dexamethasone (30uM). Differentiation Medium was changed every 2-3 for a period of 11-13 days.

To assess hepatocyte function culture medium was collected 24h after the last medium change. Functional studies were performed in the collected supernatant or in whole organoids as described in Supplemental Experimental Procedures.

Transplantation

We used a modified version of the protocol used by Guo et al. (Guo et al., 2002). In short, female BALB/c nude mice (around 7 weeks of age) were pretreated with two injections of 70 mg/kg Retrorsine (Sigma) at 30 and 14 days before transplantation. One day prior to transplantation, mice received 0.5 ml/kg CCl₄ and 50 mg/animal anti-asialo GM1 (Wako pure chemical industries) via IP injection. Furthermore, animals received 7.5 ug/ml FK506 in drinking water until the end of the experiment, due to the reported positive effects on liver regeneration (He et al., 2010). On the day of transplantation, mice were anaesthetized and suspensions of 1-2x10⁶ human liver organoid cells derived from 4 independent donors (p6 to p10) were injected intrasplenically. Transplanted mice received weekly injections of 50 mg/animal anti-asialo GM1 (Wako pure chemical industries) to deplete NK cells. To monitor the transplantation state, blood samples were taken in regular intervals from the tail vein and analyzed for the presence of human albumin and human α 1-antitrypsin using respective human specific ELISAs (Assaypro).

Karyotyping and Genetic stability analysis

Organoid cultures in exponential growing phase were incubated for 16 hours with 0.05 μ g/ml colcemid (Gibco). Then, cultures were dissociated into single cells using TrypLE express (Gibco) and processed using standard karyotyping protocols.

DNA libraries for WGS analysis were generated from 1 μ g of genomic DNA using standard protocols (Illumina). The libraries were sequenced with paired-end (2 x 100 bp) runs using Illumina HiSeq 2500 sequencers to a minimal depth of 30 x base coverage (average depth of ~ 36.9 x base coverage). As reference sample, liver biopsies was sequenced to equal depth for the different donors. Analysis of the sequence reads, calling of CNVs and base substitutions are described in detail in Supplemental Experimental Procedures. The data for the whole genome sequencing were deposited to the EMBL European Nucleotide Archive, accession number ERP005929.

Immunohistochemistry, immunofluorescence and Image analysis

Tissues and organoids were fixed o/n with formalin or 4% PFA respectively, and stained and imaged as described in Supplemental Experimental Procedures.

A1AT-D functional experiments

Elastase inhibition assay, and detection of phosphorylated of eIF2 α were performed as described in Supplemental Experimental Procedures.

Microarray

For the expression analysis of human liver cultures, total RNA was isolated from liver biopsies or from organoids cultures grown in our defined medium, using Qiagen RNAase kit following manufacture's instructions. Five hundred ng of total RNA were labeled with low RNA Input Linear Amp kit (Agilent Technologies, Palo Alto, CA). Universal human Reference RNA (Agilent) was differentially labeled and hybridized to the tissue or cultured samples. A 4X 44 K Agilent Whole Human Genome dual colour Microarray (G4122F) was used. Labeling, hybridization, and washing were performed according to Agilent guidelines.

Microarray signal and background information were retrieved using Feature Extraction software (V.9.5.3, Agilent Technologies). The hierarchical clustering analysis was performed in whole liver tissue lysate or organoid arrays. A cut-off of 3-fold differentially expressed was used for the clustering analysis. GEO accession number pending.

Data analysis

All values are represented as mean \pm standard error of the mean (S.E.M.). Man-Whitney non-parametric test was used. $p < 0.05$ was considered statistically significant. In all cases data from at least 3 independent experiments was used. All calculations were performed using SPSS package.

Author's contribution

MH, HG and HC designed, and together with KH performed and analyzed experiments. MH developed and characterized the human liver culture system. MH, RvB, EC and HC designed the genetic studies. MH, HG designed and MH, HG and KH performed A1AT experiments. MH, HG and HC designed and HG and KH performed ductal origin, transplantation and AGS experiments. RvB performed the genetic stability studies, supervised the next-gen sequencing and set up the filtering pipeline. FB adjusted and applied pipeline. JdL performed the CNV analysis. MH, MvW, RH, SF, SJB, HK performed functional in vitro experiments and analyzed the data. MvdW and NS performed FACS. MMAV, JNMI and LvdL provided METC and human liver donor and patient material. EN and RRGV provided METC. RRGV, helpful discussions. SS and EE provided isolated hepatocytes. MH, HG, RvB, EC and HC wrote the manuscript. All authors commented on the manuscript.

Acknowledgements

We thank The Hubrecht Imaging Center for imaging assistance and the Genome Diagnostics laboratory of the UMC-Utrecht for help with the Karyotype analysis. We also thank Lara Elshove, Prof. Herold Metselaar, Petra de Ruiter, and the Erasmus MC liver explantation student team for their help with obtaining the liver biopsies. This work was supported by grants to MH (EU/236954) and to HC (The United European Gastroenterology Federation (UEGF) Research Prize 2010, EU/232814-StemCellMark and NWO/116002008). MH is supported by The Wellcome Trust Sir Henry Dale fellowship. The Rspo cell line was kindly provided by Dr. Calvin Kuo.

References

- Abyzov, A., Mariani, J., Palejev, D., Zhang, Y., Haney, M.S., Tomasini, L., Ferrandino, A.F., Rosenberg Belmaker, L.A., Szekely, A., Wilson, M., *et al.* (2012). Somatic copy number mosaicism in human skin revealed by induced pluripotent stem cells. *Nature* *492*, 438-442.
- Asrani, S.K., Larson, J.J., Yawn, B., Therneau, T.M., and Kim, W.R. (2013). Underestimation of liver-related mortality in the United States. *Gastroenterology* *145*, 375-382 e371-372.
- Baker, D.E., Harrison, N.J., Maltby, E., Smith, K., Moore, H.D., Shaw, P.J., Heath, P.R., Holden, H., and Andrews, P.W. (2007). Adaptation to culture of human embryonic stem cells and oncogenesis in vivo. *Nat Biotechnol* *25*, 207-215.
- Barker, N., Huch, M., Kujala, P., van de Wetering, M., Snippert, H.J., van Es, J.H., Sato, T., Stange, D.E., Begthel, H., van den Born, M., *et al.* (2010). Lgr5(+ve) stem cells drive self-renewal in the stomach and build long-lived gastric units in vitro. *Cell Stem Cell* *6*, 25-36.
- Barker, N., van Es, J.H., Kuipers, J., Kujala, P., van den Born, M., Cozijnsen, M., Haegbarth, A., Korving, J., Begthel, H., Peters, P.J., *et al.* (2007). Identification of stem cells in small intestine and colon by marker gene Lgr5. *Nature* *449*, 1003-1007.
- Bayart, E., and Cohen-Haguener, O. (2013). Technological overview of iPS induction from human adult somatic cells. *Curr Gene Ther* *13*, 73-92.
- Bigorgne, A.E., Farin, H.F., Lemoine, R., Nizar, M., Lambert, N., Gil, M., Schulz, A., Philippet, P., Schlessner, P., Abrahamsen, T.G., *et al.* (2014). TTC7A mutations disrupt intestinal epithelial apical-basal polarity. *J Clin Invest* *124*, 328-337.
- Cairns, J. (1975). Mutation selection and the natural history of cancer. *Nature* *255*, 197-200.
- Carmon, K.S., Gong, X., Lin, Q., Thomas, A., and Liu, Q. (2011). R-spondins function as ligands of the orphan receptors LGR4 and LGR5 to regulate Wnt/beta-catenin signaling. *Proc Natl Acad Sci USA* *108*, 11452-11457.
- Casciano, D.A. (2000). Development and utilization of primary hepatocyte culture systems to evaluate metabolism, DNA binding, and DNA repair of xenobiotics. *Drug Metab Rev* *32*, 1-13.
- Cheng, L., Hansen, N.F., Zhao, L., Du, Y., Zou, C., Donovan, F.X., Chou, B.K., Zhou, G., Li, S., Dowey, S.N., *et al.* (2012). Low incidence of DNA sequence variation in human induced pluripotent stem cells generated by nonintegrating plasmid expression. *Cell Stem Cell* *10*, 337-344.
- Choi, T.Y., Ninov, N., Stainier, D.Y., and Shin, D. (2014). Extensive conversion of hepatic biliary epithelial cells to hepatocytes after near total loss of hepatocytes in zebrafish. *Gastroenterology* *146*, 776-788.
- de Lau, W., Barker, N., Low, T.Y., Koo, B.K., Li, V.S., Teunissen, H., Kujala, P., Haegbarth, A., Peters, P.J., van de Wetering, M., *et al.* (2011). Lgr5 homologues associate with Wnt receptors and mediate R-spondin signalling. *Nature* *476*, 293-297.
- Dekkers, J.F., Wiegerinck, C.L., de Jonge, H.R., Bronsveld, I., Janssens, H.M., de Winter-de Groot, K.M., Brandsma, A.M., de Jong, N.W., Bijvelds, M.J., Scholte, B.J., *et al.* (2013). A functional CFTR assay using primary cystic fibrosis intestinal organoids. *Nat Med* *19*, 939-945.

Dooley, S., and ten Dijke, P. (2012). TGF-beta in progression of liver disease. *Cell and Tissue Res* 347, 245-256.

Dorrell, C., Erker, L., Schug, J., Kopp, J.L., Canaday, P.S., Fox, A.J., Smirnova, O., Duncan, A.W., Finegold, M.J., Sander, M., *et al.* (2011). Prospective isolation of a bipotential clonogenic liver progenitor cell in adult mice. *Genes & Dev* 25, 1193-1203.

Duncan, A.W., Dorrell, C., and Grompe, M. (2009). Stem cells and liver regeneration. *Gastroenterology* 137, 466-481.

Fairbanks, K.D., and Tavill, A.S. (2008). Liver disease in alpha 1-antitrypsin deficiency: a review. *Am J Gastroenterol* 103, 2136-2141; quiz 2142.

Francis, H., Glaser, S., Ueno, Y., Lesage, G., Marucci, L., Benedetti, A., Taffetani, S., Marzioni, M., Alvaro, D., Venter, J., *et al.* (2004). cAMP stimulates the secretory and proliferative capacity of the rat intrahepatic biliary epithelium through changes in the PKA/Src/MEK/ERK1/2 pathway. *J Hepatol* 41, 528-537.

Furuyama, K., Kawaguchi, Y., Akiyama, H., Horiguchi, M., Kodama, S., Kuhara, T., Hosokawa, S., Elbahrawy, A., Soeda, T., Koizumi, M., *et al.* (2011). Continuous cell supply from a Sox9-expressing progenitor zone in adult liver, exocrine pancreas and intestine. *Nature genetics* 43, 34-41.

Geisler, F., Nagl, F., Mazur, P.K., Lee, M., Zimmer-Strobl, U., Strobl, L.J., Radtke, F., Schmid, R.M., and Siveke, J.T. (2008). Liver-specific inactivation of Notch2, but not Notch1, compromises intrahepatic bile duct development in mice. *Hepatology* 48, 607-616.

Gore, A., Li, Z., Fung, H.L., Young, J.E., Agarwal, S., Antosiewicz-Bourget, J., Canto, I., Giorgetti, A., Israel, M.A., Kiskinis, E., *et al.* (2011). Somatic coding mutations in human induced pluripotent stem cells. *Nature* 471, 63-67.

Gramignoli, R., Green, M.L., Tahan, V., Dorko, K., Skvorak, K.J., Marongiu, F., Zao, W., Venkataramanan, R., Ellis, E.C., Geller, D., *et al.* (2012). Development and application of purified tissue dissociation enzyme mixtures for human hepatocyte isolation. *Cell Transplant* 21, 1245-1260.

Guo, D., Fu, T., Nelson, J.A., Superina, R.A., and Soriano, H.E. (2002). Liver repopulation after cell transplantation in mice treated with retrorsine and carbon tetrachloride. *Transplantation* 73, 1818-1824.

Hattoum, A., Rubin, E., Orr, A., and Michalopoulos, G.K. (2013). Expression of hepatocyte epidermal growth factor receptor, FAS and glypican 3 in EpCAM-positive regenerative clusters of hepatocytes, cholangiocytes, and progenitor cells in human liver failure. *Hum Pathol* 44, 743-749.

He, Z., Zhang, H., Zhang, X., Xie, D., Chen, Y., Wangenstein, K.J., Ekker, S.C., Firpo, M., Liu, C., Xiang, D., *et al.* (2010). Liver xeno-repopulation with human hepatocytes in Fah^{-/-} Rag2^{-/-} mice after pharmacological immunosuppression. *Am J Pathol* 177, 1311-1319.

Huch, M., Bonfanti, P., Boj, S.F., Sato, T., Loomans, C.J., van de Wetering, M., Sojoodi, M., Li, V.S., Schuijers, J., Gracanin, A., *et al.* (2013a). Unlimited in vitro expansion of adult bi-potent pancreas progenitors through the Lgr5/R-spondin axis. *The EMBO J* 32, 2708-2721.

- Huch, M., Dorrell, C., Boj, S.F., van Es, J.H., Li, V.S., van de Wetering, M., Sato, T., Hamer, K., Sasaki, N., Finegold, M.J., *et al.* (2013b). In vitro expansion of single Lgr5⁺ liver stem cells induced by Wnt-driven regeneration. *Nature* 494, 247-250.
- Hussein, S.M., Batada, N.N., Vuoristo, S., Ching, R.W., Autio, R., Narva, E., Ng, S., Sourour, M., Hamalainen, R., Olsson, C., *et al.* (2011). Copy number variation and selection during reprogramming to pluripotency. *Nature* 471, 58-62.
- Jung, P., Sato, T., Merlos-Suarez, A., Barriga, F.M., Iglesias, M., Rossell, D., Auer, H., Gallardo, M., Blasco, M.A., Sancho, E., *et al.* (2011). Isolation and in vitro expansion of human colonic stem cells. *Nat Med* 17, 1225-1227.
- Kamath, B.M., Spinner, N.B., and Rosenblum, N.D. (2013). Renal involvement and the role of Notch signalling in Alagille syndrome. *Nat Rev Nephrol* 9, 409-418.
- Laurent, L.C., Ulitsky, I., Slavin, I., Tran, H., Schork, A., Morey, R., Lynch, C., Harness, J.V., Lee, S., Barrero, M.J., *et al.* (2011). Dynamic changes in the copy number of pluripotency and cell proliferation genes in human ESCs and iPSCs during reprogramming and time in culture. *Cell Stem Cell* 8, 106-118.
- Lawless, M.W., Mankan, A.K., Gray, S.G., and Norris, S. (2008). Endoplasmic reticulum stress--a double edged sword for Z alpha-1 antitrypsin deficiency hepatotoxicity. *The international journal of biochemistry & cell biology* 40, 1403-1414.
- Liang, G., and Zhang, Y. (2013). Genetic and epigenetic variations in iPSCs: potential causes and implications for application. *Cell Stem Cell* 13, 149-159.
- Lund, R.J., Narva, E., and Lahesmaa, R. (2012). Genetic and epigenetic stability of human pluripotent stem cells. *Nat Rev Genet* 13, 732-744.
- Martins-Taylor, K., Nisler, B.S., Taapken, S.M., Compton, T., Crandall, L., Montgomery, K.D., Lalande, M., and Xu, R.H. (2011). Recurrent copy number variations in human induced pluripotent stem cells. *Nat Biotechnol* 29, 488-491.
- Massague, J., Blain, S.W., and Lo, R.S. (2000). TGFbeta signaling in growth control, cancer, and heritable disorders. *Cell* 103, 295-309.
- Massague, J., Seoane, J., and Wotton, D. (2005). Smad transcription factors. *Genes & Dev* 19, 2783-2810.
- Mayshar, Y., Ben-David, U., Lavon, N., Biancotti, J.C., Yakir, B., Clark, A.T., Plath, K., Lowry, W.E., and Benvenisty, N. (2010). Identification and classification of chromosomal aberrations in human induced pluripotent stem cells. *Cell Stem Cell* 7, 521-531.
- McCright, B., Lozier, J., and Gridley, T. (2002). A mouse model of Alagille syndrome: Notch2 as a genetic modifier of Jag1 haploinsufficiency. *Development* 129, 1075-1082.
- Michalopoulos, G.K. (2013). Principles of liver regeneration and growth homeostasis. *Compr Physiol* 3, 485-513.
- Michalopoulos, G.K. (2014). The liver is a peculiar organ when it comes to stem cells. *The Am J Pathol* 184, 1263-1267.
- Mitaka, T. (1998). The current status of primary hepatocyte culture. *Int J Exp Pathol* 79, 393-409.

- Pera, M.F. (2011). Stem cells: The dark side of induced pluripotency. *Nature* 471, 46-47.
- Rashid, S.T., Corbineau, S., Hannan, N., Marciniak, S.J., Miranda, E., Alexander, G., Huang-Doran, I., Griffin, J., Ahrlund-Richter, L., Skepper, J., *et al.* (2010). Modeling inherited metabolic disorders of the liver using human induced pluripotent stem cells. *J Clin Invest* 120, 3127-3136.
- Sato, T., Stange, D.E., Ferrante, M., Vries, R.G., Van Es, J.H., Van den Brink, S., Van Houdt, W.J., Pronk, A., Van Gorp, J., Siersema, P.D., *et al.* (2011). Long-term expansion of epithelial organoids from human colon, adenoma, adenocarcinoma, and Barrett's epithelium. *Gastroenterology* 141, 1762-1772.
- Sato, T., Vries, R.G., Snippert, H.J., van de Wetering, M., Barker, N., Stange, D.E., van Es, J.H., Abo, A., Kujala, P., Peters, P.J., *et al.* (2009). Single Lgr5 stem cells build crypt-villus structures in vitro without a mesenchymal niche. *Nature* 459, 262-265.
- Schaub, J.R., Malato, Y., Gormond, C., and Willenbring, H. (2014). Evidence against a Stem Cell Origin of New Hepatocytes in a Common Mouse Model of Chronic Liver Injury. *Cell Rep* 8, 933-939.
- Schmelzer, E., Zhang, L., Bruce, A., Wauthier, E., Ludlow, J., Yao, H.L., Moss, N., Melhem, A., McClelland, R., Turner, W., *et al.* (2007). Human hepatic stem cells from fetal and postnatal donors. *J Exp Med* 204, 1973-1987.
- Schmierer, B., and Hill, C.S. (2007). TGFbeta-SMAD signal transduction: molecular specificity and functional flexibility. *Nat Rev Mol Cell Biol* 8, 970-982.
- Schwank, G., Koo, B.K., Sasselli, V., Dekkers, J.F., Heo, I., Demircan, T., Sasaki, N., Boymans, S., Cuppen, E., van der Ent, C.K., *et al.* (2013). Functional repair of CFTR by CRISPR/Cas9 in intestinal stem cell organoids of cystic fibrosis patients. *Cell Stem Cell* 13, 653-658.
- Shan, J., Schwartz, R.E., Ross, N.T., Logan, D.J., Thomas, D., Duncan, S.A., North, T.E., Goessling, W., Carpenter, A.E., and Bhatia, S.N. (2013). Identification of small molecules for human hepatocyte expansion and iPS differentiation. *Nat Chem Biol* 9, 514-520.
- Shin, S., Walton, G., Aoki, R., Brondell, K., Schug, J., Fox, A., Smirnova, O., Dorrell, C., Erker, L., Chu, A.S., *et al.* (2011). Foxl1-Cre-marked adult hepatic progenitors have clonogenic and bilineage differentiation potential. *Genes & Dev* 25, 1185-1192.
- Stoller, J.K., and Aboussouan, L.S. (2005). Alpha1-antitrypsin deficiency. *Lancet* 365, 2225-2236.
- Sugimoto, H., Yang, C., LeBleu, V.S., Soubasakos, M.A., Giraldo, M., Zeisberg, M., and Kalluri, R. (2007). BMP-7 functions as a novel hormone to facilitate liver regeneration. *FASEB J* 21, 256-264.
- Verrecchia, F., Chu, M.L., and Mauviel, A. (2001). Identification of novel TGF-beta /Smad gene targets in dermal fibroblasts using a combined cDNA microarray/promoter transactivation approach. *J Biol Chem* 276, 17058-17062.
- Vilarinho, S., and Lifton, R.P. (2012). Liver transplantation: from inception to clinical practice. *Cell* 150, 1096-1099.

Wandel, C., Bocker, R., Bohrer, H., Browne, A., Rugheimer, E., and Martin, E. (1994). Midazolam is metabolized by at least three different cytochrome P450 enzymes. *Br J Anaesth* 73, 658-661.

Wiegerinck, C.L., Janecke, A.R., Schneeberger, K., Vogel, G.F., van Haften-Visser, D.Y., Escher, J.C., Adam, R., Thoni, C.E., Pfaller, K., Jordan, A.J., *et al.* (2014). Loss of Syntaxin 3 Causes Variant Microvillus Inclusion Disease. *Gastroenterology*. *in press* doi:10.1053/j.gastro.2014.04.002

Wu, A.L., Coulter, S., Liddle, C., Wong, A., Eastham-Anderson, J., French, D.M., Peterson, A.S., and Sonoda, J. (2011). FGF19 regulates cell proliferation, glucose and bile acid metabolism via FGFR4-dependent and independent pathways. *PLoS one* 6, e17868.

Xu, J., Lamouille, S., and Derynck, R. (2009). TGF-beta-induced epithelial to mesenchymal transition. *Cell Res* 19, 156-172.

Yanger, K., Knigin, D., Zong, Y., Maggs, L., Gu, G., Akiyama, H., Pikarsky, E., and Stanger, B.Z. (2014). Adult hepatocytes are generated by self-duplication rather than stem cell differentiation. *Cell Stem Cell* 15, 340-349.

Yanger, K., Zong, Y., Maggs, L.R., Shapira, S.N., Maddipati, R., Aiello, N.M., Thung, S.N., Wells, R.G., Greenbaum, L.E., and Stanger, B.Z. (2013). Robust cellular reprogramming occurs spontaneously during liver regeneration. *Genes & Dev* 27, 719-724.

Yoon, S.M., Gerasimidou, D., Kuwahara, R., Hytioglou, P., Yoo, J.E., Park, Y.N., and Theise, N.D. (2011). Epithelial cell adhesion molecule (EpCAM) marks hepatocytes newly derived from stem/progenitor cells in humans. *Hepatology* 53, 964-973.

Figure Legends

Figure 1: Human liver biopsies grow long term as epithelial organoids from ductal origin

Human liver cells were isolated from biopsies from liver donor material by collagenase dissociation. Tissues were dissociated to single cell and 3000 or 10000 cells were seeded per well in a 48well plate in different culture conditions as indicated on the Figure. (A) Scheme of the experimental protocol. (B) Cells were seeded in different culture conditions as follows: mouse liver culture medium (ERFHNic) or medium supplemented with A8301 or A8301 and Forskolin (FSK) as indicated and organoids were allowed to grow. The cultures were split every week 7-10 days at a ratio of 1:4 -1:6 dilution. Cells started to proliferate however, the cultures grown in mouse medium or medium supplemented with A8301 only arrested proliferation after some weeks in culture and could not be expanded any further as indicated in the graph. Supplementing the culture medium with A8301 combined with FSK significantly increased the expansion efficiency of the cultures which have been able to grow for >18 passages at a split ratio of 1:4-1:6 every 7-10 days for >5 months. Experiments were performed in triplicate. Each bar indicates a different donor starting material. (C) DIC images of organoids treated with mouse liver medium +A8301 and supplemented (right panel) or not (left panel) with FSK. (D) Graph indicating the % of colony formation efficiency in cultures seeded in the presence or absence of A8301 and or FSK. Experiments were performed in triplicate. Five different donor derived cultures were counted. Results are expressed as mean \pm SEM of 5 independent experiments. (E-G) To quantify the proliferation capacity of the

human liver cultures, expansion ratios, *in vitro* growth curves and EdU incorporation, at early and late passages, were analyzed in human liver cultures grown in complete medium (ENRFHNic + A8301 and FSK). (E-F) Cell numbers were counted by Trypan blue exclusion at the indicated time points, in at least triplicates of 3 independent human donor materials. The cultures followed an exponential growth curve within each time window analyzed. Graphs illustrate the number of cells counted per well at each passage from P1-P4 (E) to P16-P18 (F). The doubling time, or amount of time the culture needs to double its original size, was calculated as described in Supplemental Experimental Procedures. Note that the doubling time was essentially maintained once the culture had started to expand (from day 16 onwards). (G) Similarly, EdU incorporation was still detected at late passages, again indicating that the cells maintain their proliferation potential *in vitro* after long-term culturing. (H) Human liver cell suspensions were separated into EpCAM⁺ ductal cells and larger, EpCAM⁻ hepatocytes (for exact gating strategy see Figure S2C). Identity of the populations was confirmed by cytopins and subsequent IF staining for Albumin and KRT19. Sorted cells were seeded into matrigel and grown for 14 days into organoids. Organoids were exclusively derived from EpCAM⁺ ductal cells. See also Figure S1 and Figure S2.

Figure 2: Human organoids are genetically stable after months of expansion in culture

Genetic stability of human liver cultures was analyzed in clonally grown cultures that had been expanded for > 3 months (~120 days) in our complete human liver medium. (A) Human liver biopsies were dissociated into single cells and clonal cultures were obtained by seeding sorted cells at a ratio of 1 cell per well. As illustrated, cells quickly proliferated and expanded in culture. DIC images of growing single cells from human liver cultures. Magnifications: 40x (days 0-10), 4x (day 20-onwards). (B-D) Genetic stability of the human liver organoid cultures clonally expanded long-term *in vitro*. (B) Schematic overview of the experimental setup. Two independent donor liver biopsies were minced and cultured for one week. Subsequently, single liver stem cells were isolated and clonally expanded to obtain two independent organoid cultures per donor (culture A and culture B). These cultures were subjected to long-term expansion after which a second clonal expansion step was performed. The resulting organoid cultures were subjected to whole genome sequencing (WGS) analysis. To obtain all somatic variation present in the cultures, variants were filtered for presence in the original biopsy. To determine the effect of long-term culturing on genomic stability, somatic variation was filtered for presence in earlier passages. (C) Number of somatic base substitution observed in the different organoid cultures. The pie-chart indicates the percentage of the genome that was surveyed per donor. The right panels indicate the absolute numbers of base substitution observed in the surveyed part of the genome. Indicated are the total number of somatic base substitutions per culture and the number induced by long-term culturing. (D) Effect of somatic base substitutions on protein-coding DNA. Left panels indicate the total number of somatic base substitutions per donor and the left panel indicates the part that affects protein-coding DNA. See also Figure S3.

Figure 3. Structural variation in human liver organoids.

(A) Representative karyotyping image of organoids cultured for 16 days (P1) and 90 days (P14) illustrating a normal chromosomal count (n=46). No major chromosomal aberrations were observed in any of the samples analyzed (n=15). Detailed chromosomal counts for different donors are shown in supplemental Figure S4. (B) Read-depth analysis of whole genome sequencing data over the different chromosomes for the biopsy (upper panel) and organoid culture A (lower panel) that were derived from donor 2. Read-depth was corrected

for GC content and normalized for genome coverage. Grey dotted lines indicate log₂ values associated with a gain or deletion. (C) Copy number analysis of a region at chromosome 3 that was found to harbor a heterozygous gain in culture A of donor 2. Left panels indicate read-depth analysis of the indicated region in 5kb bins, corrected for GC content and normalized for genome coverage, of the biopsy (upper panel) and organoid culture (lower panel). Right panels show the variant allele frequencies of informative non-reference single nucleotide polymorphisms (SNPs) in the indicated region for the biopsy (upper panel) and organoid culture (lower panel). (D) Summary of the copy number analysis of the different organoid cultures of the two donors. Somatic CNVs were exclusively observed in culture A derived from donor 2, which were already present in the parental culture. See also Figure S4.

Figure 4: Human liver organoids express LGR5 and markers of the ductal and hepatocyte lineages

Gene expression was analyzed by RT-PCR (A) and immunofluorescence (B) in human liver cultures grown in our defined expansion medium as described in Experimental Procedures. (A) Gene expression was analyzed at early (EP) and late (LP) passages. Human liver cultures expressed progenitor (LGR5, SOX9), ductal (KRT19, SOX9) and hepatocyte (HNF4A) markers but they do not express albumin (ALB) while in expansion medium. Results are indicated as 2^{-dCt} (2^{ΔΔCT}). Values represent mean ± SEM of 3 independent experiments in 5 independent donor derived cultures. 2^{ΔΔCT} were calculated using the housekeeping gene GAPDH as reference gene for normalization. (B-F) Confocal images of a human liver organoid showing that the organoids are formed by epithelial derived structures positive for ECAD and the hepatocyte marker HNF4 (B), and the ductal markers (KRT19, C; KRT7, D) and SOX9 (E). Nuclei were counterstained with Hoechst. (F) Confocal images of a human liver organoid showing that the organoids are formed by epithelial derived cells positive for EPCAM (blue). The stem cell marker Lgr5 (green) was restricted to a subset of cells within the organoid, while the Wnt target gene EPHB2 (red) was broadly expressed, but co-localized with LGR5, as expected. See also Figure S5.

Figure 5: Upon Differentiation, organoid cultures upregulate hepatocyte genes

Human liver cultures were expanded for at least 1 month in culture and transferred to our differentiation medium as described in Experimental Procedures. (A) Scheme of the experimental plan. (B-C) Expression of hepatocyte genes was determined by immunofluorescence (B) or qPCR (C) 11 days later. (B) Immunofluorescence staining showing albumin (ALB, red) and zona occludens (ZO-1, green) positive cells all over the organoid, indicating that the cells start expressing hepatocyte markers. (C) qPCR analysis indicated that both, albumin and Cytochrome p450 3A4 isoform were highly expressed upon differentiation. Graphs indicate mean ± SEM of 3 independent experiments in 3 independent donor derived cultures. EM, expansion medium including FSK. DM, differentiation medium, Tissue, whole lysate from human liver. **, p<0,01 when comparing EM vs DM. (D) Whole genome transcriptome analysis of human liver cultures grown in our expansion medium (EM) or after being cultured 11 days in our defined Differentiation medium (DM). Heat map indicates cluster of genes highly expressed in liver tissue and in organoid cultures upon differentiation. Of note, this cluster contains genes essential for liver function, as the indicated in red. Green, downregulated; Red, upregulated. See also Figure S5.

Figure 6: Liver cultures exhibit hepatocyte functions *in vitro* and *in vivo*

To test whether the cells could have differentiated towards functional hepatocytes *in vitro*, we determined the ability of the cultures to retain some hepatocyte functions *in vitro*, upon differentiation. **(A)**, Glycogen accumulation was determined by PAS (Periodic-Acid Schiff) staining in organoids grown in EM or DM for 11 days. PAS positive staining (pink) was exclusively observed in the organoids after Differentiation (DM), indicating that the cells exhibit capacity to accumulate glycogen. Magnification, 10x. **(B)** LDL uptake was analyzed using Dil-ac-LDL fluorescent substrate (red) in cultures maintained in EM (left) or DM (right) for 11 days. Only cultures maintained in DM incorporated the substrate (red). Nuclei were counter-stained with DRAQ5. Scale bar, 25 μm . **(C)** Albumin production during 24h was measured in the supernatant of liver organoids. Results are expressed as mean \pm SEM of 2 independent experiments in 4 independent donor-derived cultures. **(D)** CYP3A4 activity was measured as described in methods in cultures kept in DM for 11 days. Results are expressed as RLU per ml per million cells. HEK293T cells and HepG2 cells were used as negative and positive controls respectively. Note that organoids upon DM exhibit similar the CYP3A4 activity as fresh isolated hepatocytes (see Figure S2A). Triplicates for each condition were analyzed. Results are shown as mean \pm SEM of 2 independent experiments in 4 independent donor-derived cultures. **(E)**, Midazolam metabolism is performed exclusively by functional CYP3A3/4/5 enzymes. 3 different organoid cultures from 2 different donors and HepG2 cells were plated and cultured for 11 days as described, then midazolam was added to the medium (5 μM) and after 24 hours, concentrations of 1-OH midazolam and 1-OH midazolam glucuronide were determined as described in methods. Duplicates for each condition and donor were analyzed. Results are shown as mean \pm SEM of 2 independent experiments. **(F)** Bile acid production was measured as described in methods. Results are shown as \pm SEM of 2 independent experiments in 2 independent donor-derived cultures. Duplicates for each condition and donor were analyzed. **(G)** Ammonia elimination was measured as described in methods. Results are shown as \pm SEM of n=3 independent experiments in 2 independent donor-derived cultures and are expressed as nM/h/million cells. **(H)** Retrorsine/CCl₄ treated Balbc/nude mice were transplanted with 1-2x10⁶ human liver organoid cells and sacrificed after 120 days. The presence of foci of human Albumin positive, but human KRT19 negative hepatocytes proves successful engraftment and differentiation in mouse liver. **(I)** Average serum levels of human Albumin in mouse circulation after transplantation. Results are shown as \pm SEM of 2 vehicle control animals, 2 primary hepatocyte transplanted mice and 6 human liver organoid transplanted animals. **, p<0,01 and *, p<0,05 when comparing EM vs DM. See also Figure S6.

Figure 7: Human A1AT deficiency Liver cultures as an *in vitro* disease model

(A) Representative pictures of A1AT deficient patient derived liver organoids at Passage 2 and Passage 11 (4x magnification). **(B)** ELISA measurement of Albumin secretion in supernatant from donor and A1AT deficient patient organoids in EM or after 11 days in DM. Patients and donors show a similar level of albumin release. Results are expressed as mean \pm SEM of 2 independent experiments. **(C)** A1AT deficient patient organoids were differentiated for 11 days and incubated with DiI-Ac-LDL as described in materials and methods. Fluorescence microscopy shows robust LDL uptake in patient organoids. Scale bar, 50 μm **(D)** Fold induction of Albumin and *CYP3A4* mRNA levels after 11 days of differentiation of donor and A1AT deficient patient organoids. Results are expressed as mean \pm SEM of 2 independent experiments **(E-H)** Immunohistochemistry for A1AT on liver tissue **(E/G)** and liver derived organoids from a healthy donor **(F)** and a representative A1AT deficient patient **(H)**. Arrows indicate A1AT protein aggregates in patient derived liver tissue **(G)** and

organoids **(H)**. Scale bar, 20 μm . **(H)** ELISA measurement of A1AT secretion in supernatants from Donor and patient organoids after 11 days of differentiation. Results are expressed as mean \pm SEM of 2 independent experiments. **(I)** Enzymatic measurement of Elastase inhibition by supernatants of differentiated donor and patient derived organoid cultures (as described in materials and methods). Supernatants from all 3 patients show reduced inhibition of Elastase activity. Results are expressed as mean \pm SEM of 2 independent experiments **(J)** Western blot of total lysates from donor and A1AT deficient patient organoids after 11 days of differentiation. Increased eIF2 α phosphorylation at Ser51 was detected in the 3 patients. Representative image is shown. Pat., patient. See also Figure S7.

Figure 1
[Click here to download Figure: revised Fig 1.pdf](#)

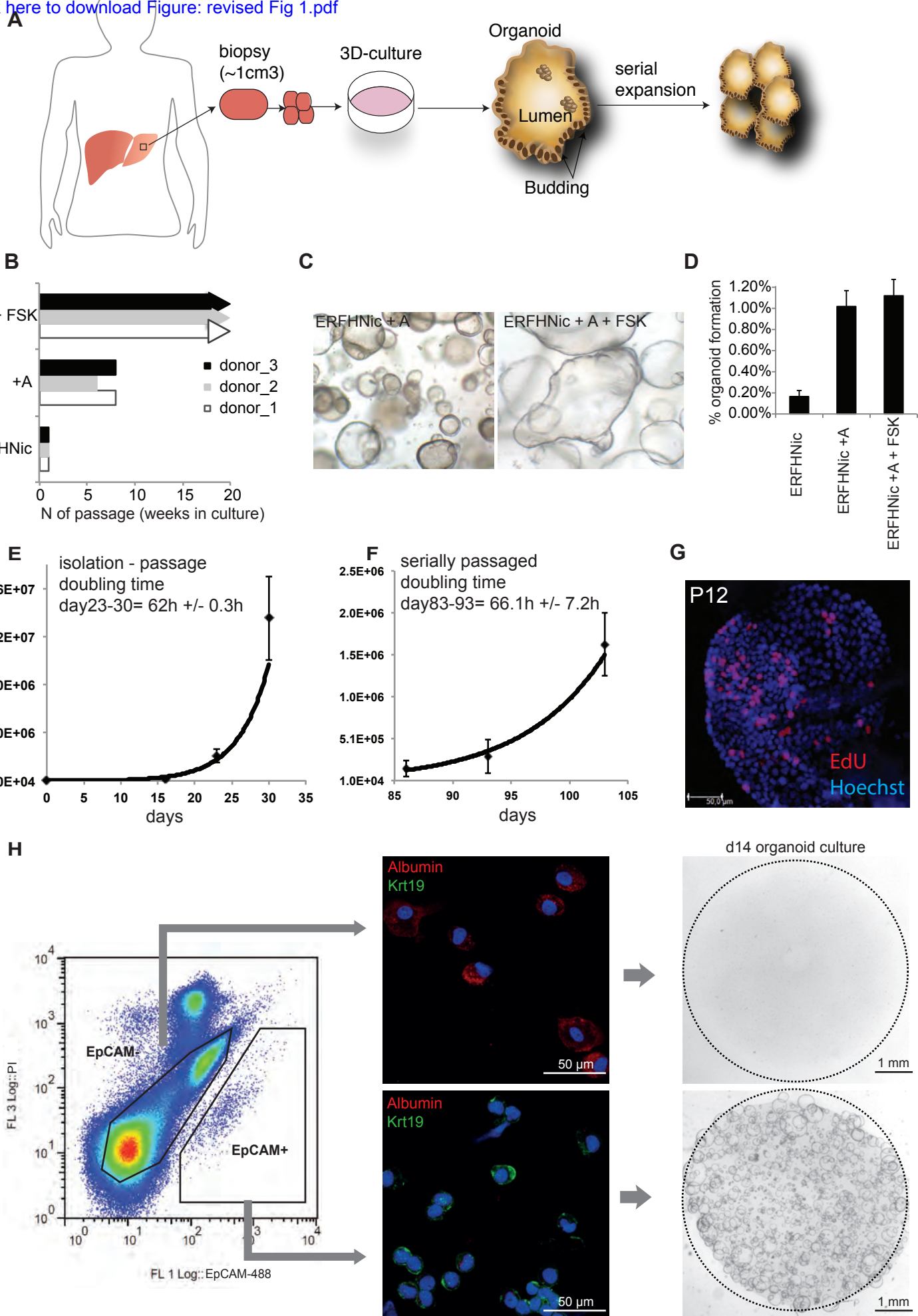


Figure 1: Human liver biopsies grow long term as epithelial organoids of ductal origin

Figure 2

[Click here to download Figure: revised Fig 2.pdf](#)

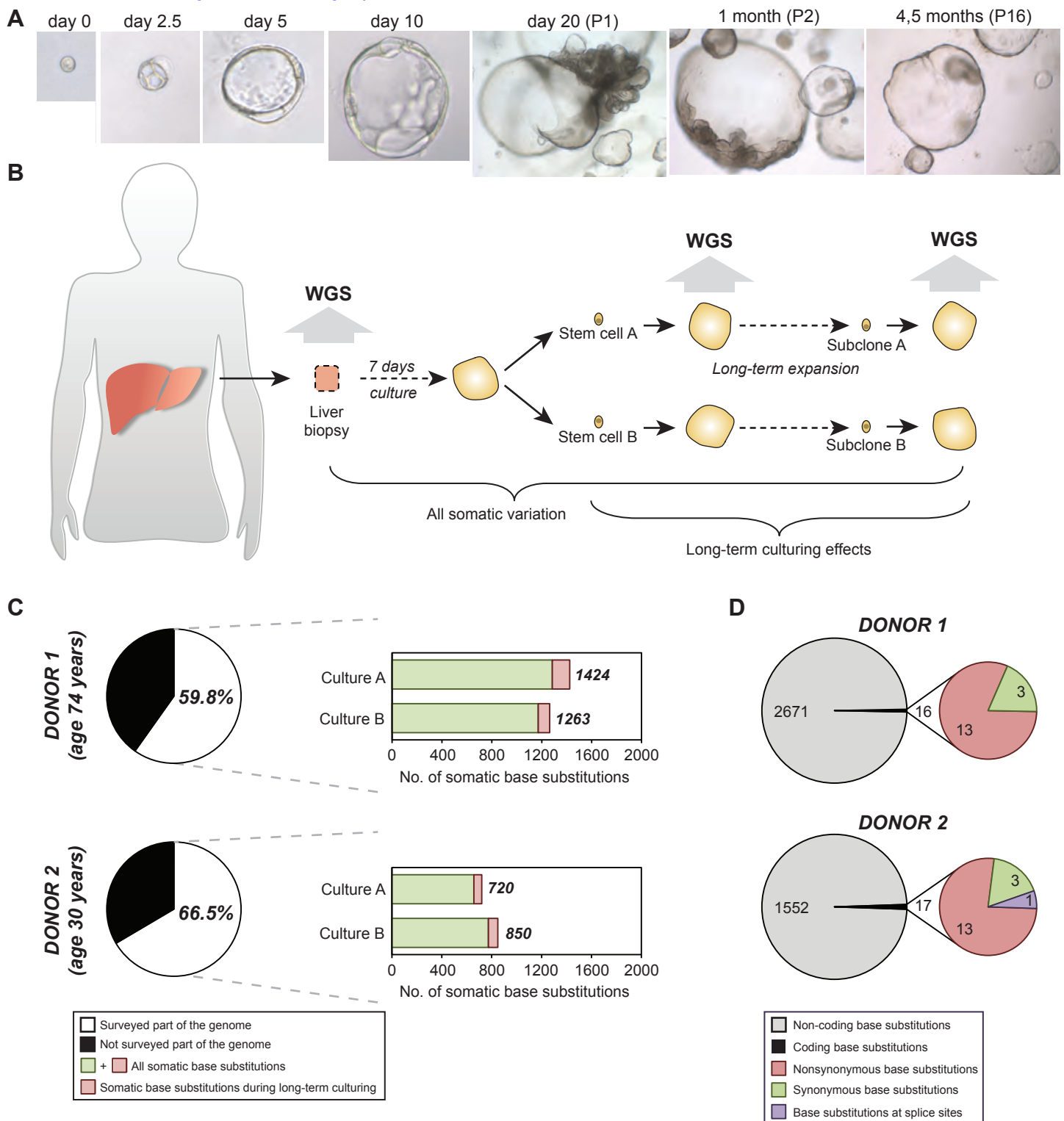


Figure 2: Human organoids are genetically stable after months of expansion in culture

Figure3
[Click here to download Figure: Fig3final.pdf](#)

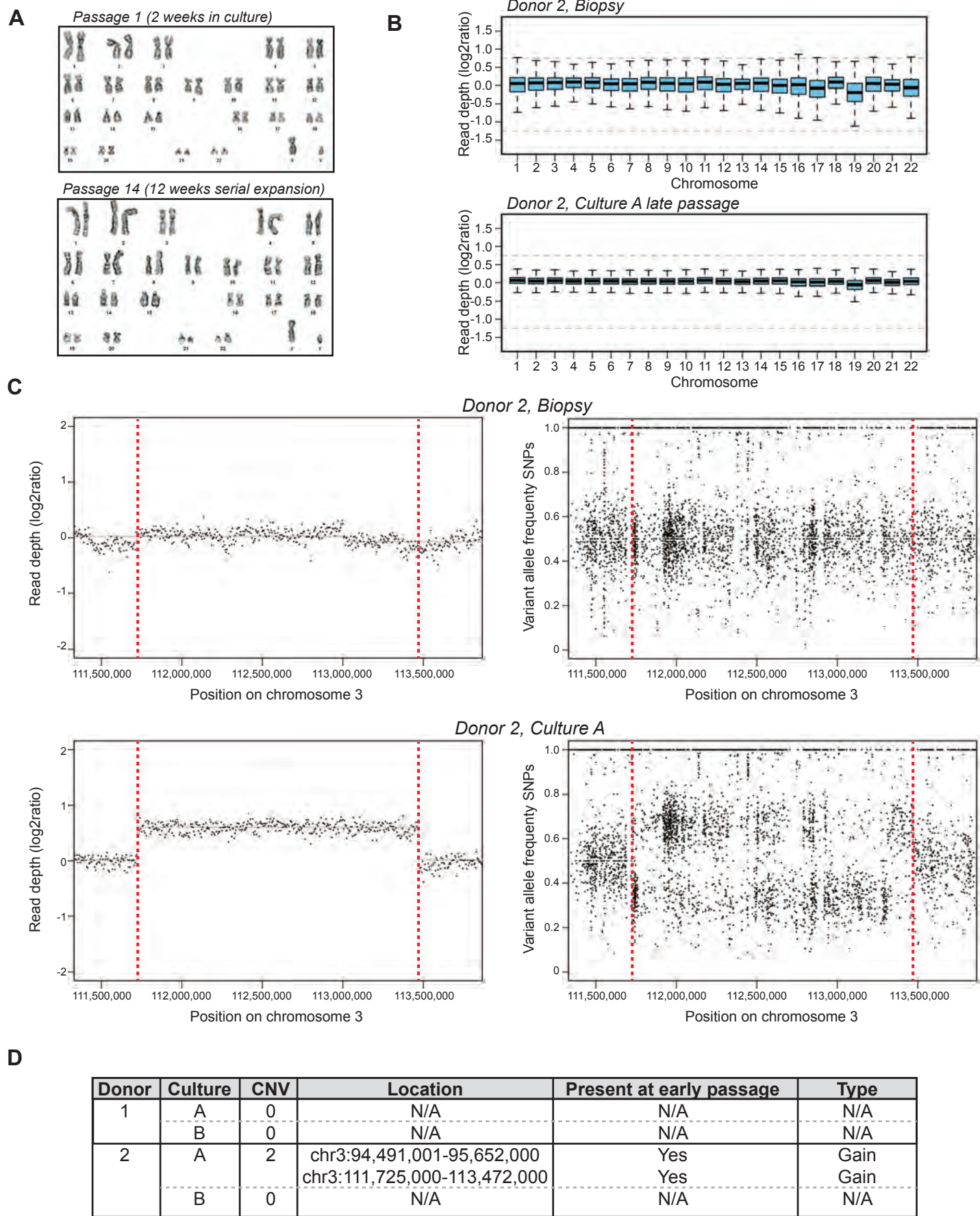


Figure 3. Structural variation in human liver organoids.

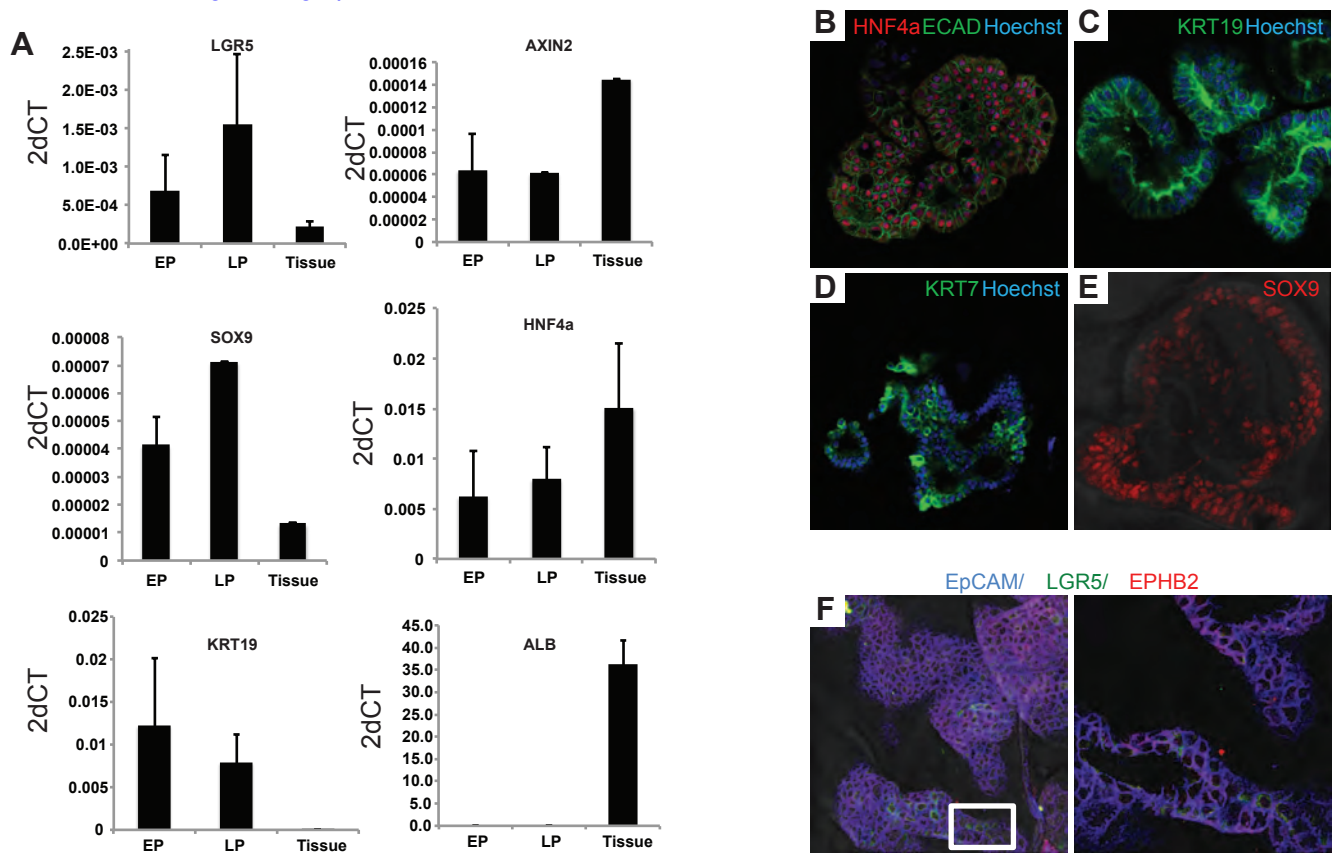


Figure 4: Human liver organoids express LGR5 and markers of the ductal and hepatocyte lineages

Figure5

[Click here to download Figure: Fig5.pdf](#)

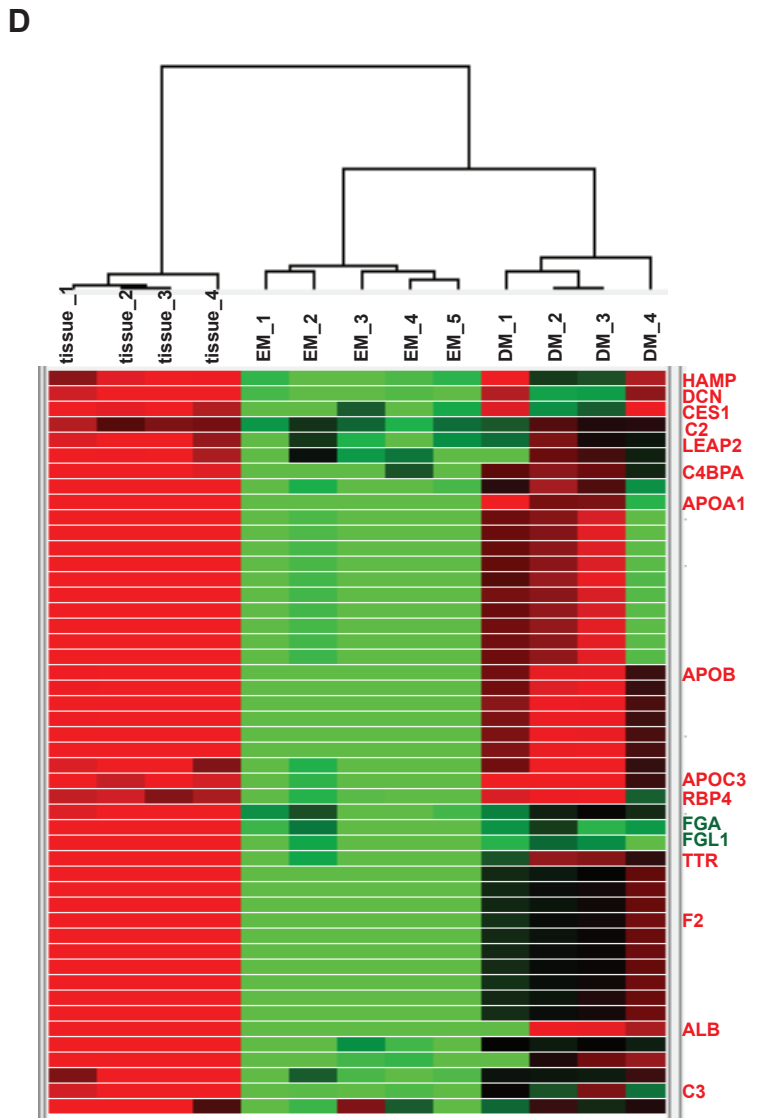
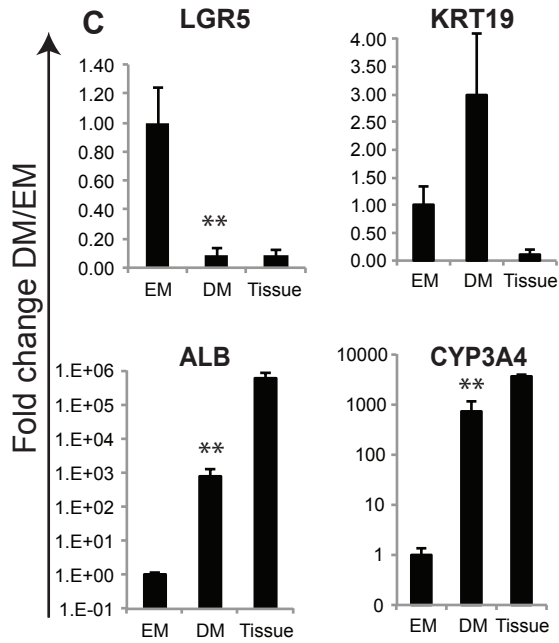
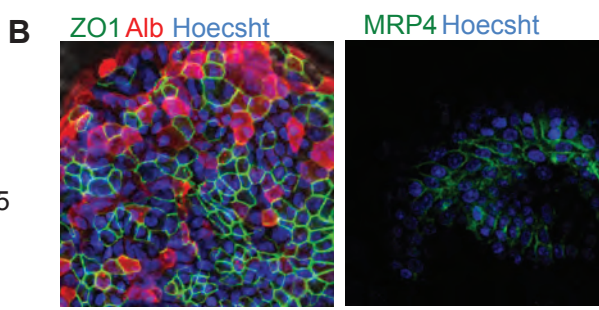
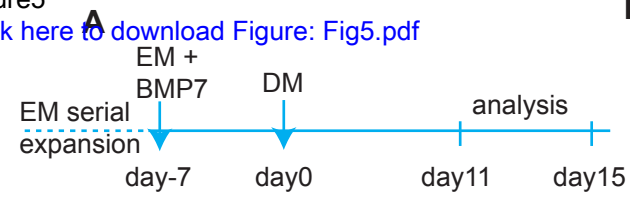


Figure 5: Upon Differentiation, organoid cultures upregulate hepatocyte genes.

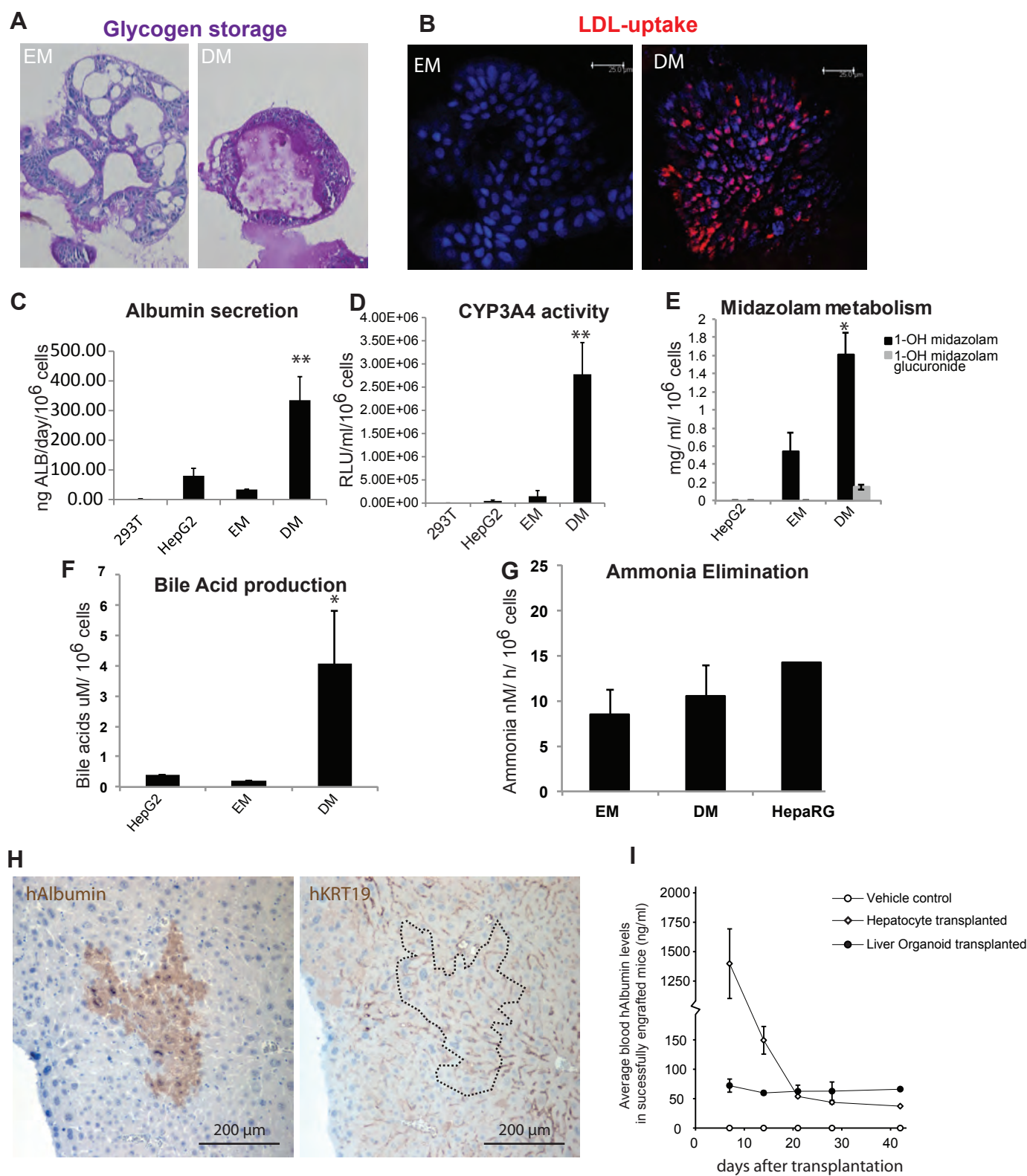


Figure 6: Liver cultures exhibit hepatocyte functions in vitro and in vivo

Figure 7

[Click here to download Figure: Fig7.pdf](#)

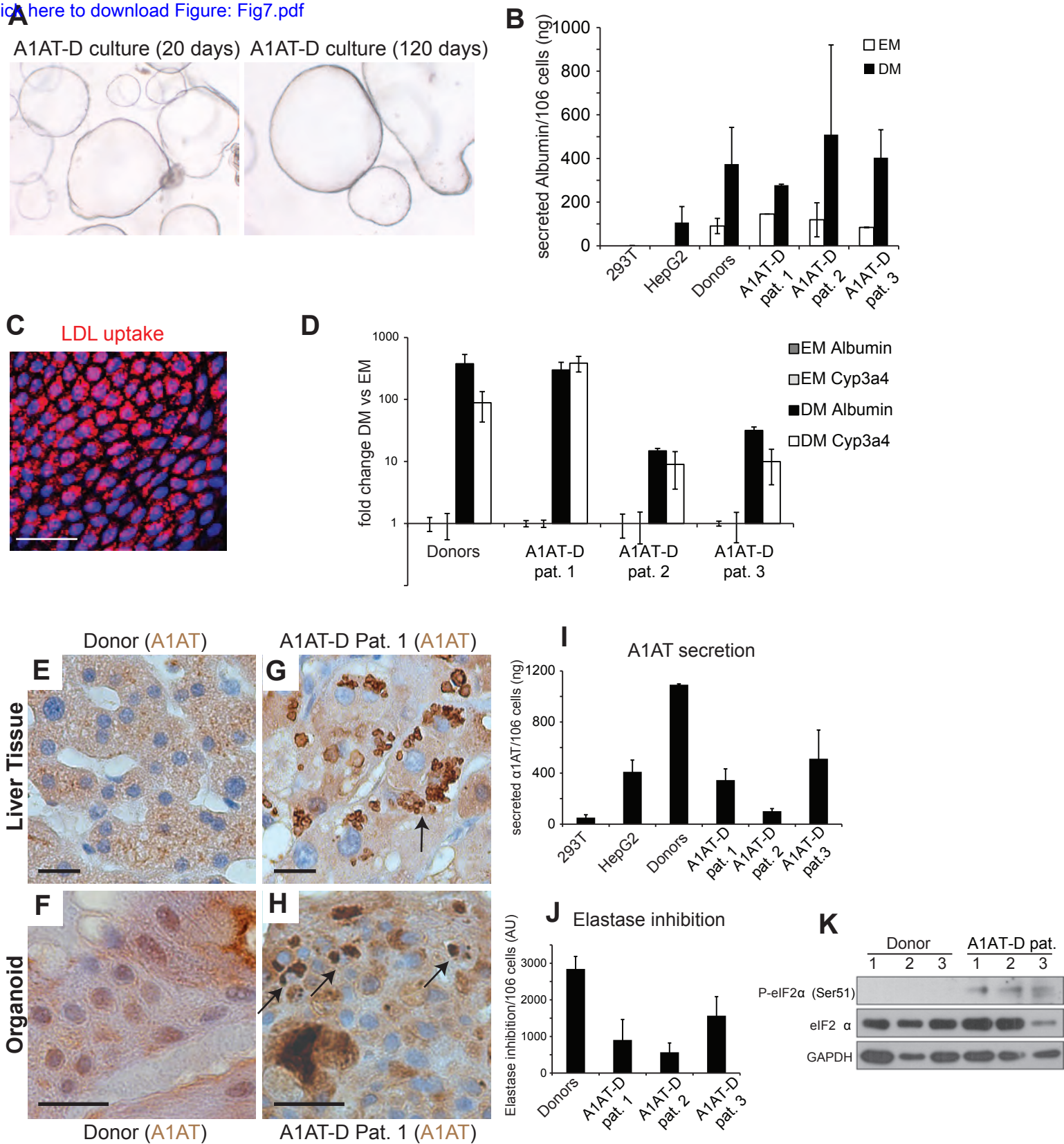


Figure 7: Human A1AT deficiency liver cultures as an in vitro disease model

Supplemental Information

Supplemental Data

Figure S1: TgFb inhibition, active Wnt signaling and cAMP activation are essential for the long term expansion of human liver cells. Related to Figure 1

Figure S2: Human liver cultures are of ductal origin. Related to Figure 1

Figure S3: Filtering steps and FNR of all sequenced samples. Related to Figure 2

Figure S4: Genetic stability of human liver stem cell cultures. Related to Figure 3

Figure S5: Analysis of organoids during expansion and upon differentiation. Related to Figure 5 and 6

Figure S6: Transplantation of human liver organoids into damaged mouse liver. Related to Figure 6.

Figure S7: Organoids from A1AT-Deficiency and AGS patients mimic disease phenotypes in vitro. Related to Figure 7.

Table S1: List of tested compounds. Related to Figure 1

List of all the compounds tested for their capacity to enhance human liver culture proliferation, long-term maintenance or differentiation. Human liver cultures were seeded in ERFHNic medium supplemented with A8301 and the compound indicated on the list. Seeding efficiency and capacity to expand long-term the cultures was evaluated. Green, the compound supports human liver growth. Red, the compound has a negative effect on the culture. Absence of color, the compound does not affect either way.

Table S2: Human material cultured. Related to Figure 1-7.

Patient and donor information from the cultured material. When available, A1AT protein serum levels are listed

Table S3: List of mutated genes with non-synonymous mutations found after WGS analysis. Related to Figure 2

Table S4: List of primers used. Related to Experimental Procedures

Table S5: List of antibodies used. Related to Experimental Procedures

Supplemental Experimental Procedures

Human liver isolation

Liver cells were isolated by collagenase digestion as follows: tissue (0.5-1cm³) was minced, rinsed 2x with DMEM (Gibco) 1%FCS and incubated with the digestion solution (2.5 mg/ml collagenase D (Roche) + 0.1 mg/ml DNase I (Sigma) in EBSS (Hyclone, ThermoFisher), for 20-40 at 37°C. The digestion was stopped by adding cold DMEM 1%FCS and the suspension was then filtered through a 70 um Nylon cell strainer and spun 5 min at 300-400g.

The pellet was resuspended in DMEM 1%FCS and kept cold. Any material retained on the strainer was further digested for 10 min in Accutase (Gibco) at 37C. Then, the digestion was stopped and the cells were collected as before. The different fractions (collagenase and accutase) were seeded and cultured as described in Experimental Procedures.

***In vitro* growth curves**

Expansion ratios were calculated from human liver cultures as follows: 3×10^3 cells were grown in our defined medium for 7 or 10 days. Then, the cultures were dissociated by incubation with TrypLE Express (Gibco) until single cells. Cell numbers were counted by trypan blue exclusion at the indicated time points. From the basic formula of the exponential curve $y(t) = y_0 \times e^{(\text{growth rate} \times t)}$ (y = cell numbers at final time point; y_0 = cell numbers at initial time point; t = time) we derived the growth rate. Then, the doubling time was calculated as doubling time = $\ln(2)/\text{growth rate}$ for each time window analyzed.

Isolation of EpCAM+ cells from primary human liver

Human liver cells were isolated according to standard protocol at the liver cell laboratory at the unit for transplantation surgery, CLINTEC, Karolinska Institute. Cell suspensions were shipped overnight on ice. Suspensions were diluted in 2 volumes of cold Advanced DMEM/F12 (Gibco) and washed 3 times in the same medium. Viable cells were counted with Trypan blue and split into 3 parts for EpCAM sorting, Percoll purification (see Hepatocyte Percoll purification) and direct seeding into matrigel. For sorting, liver cells were stained with 1:100 Anti-Human CD326 (EpCAM) Alexa Fluor® 488 (eBioscience) for 30 minutes at 4°C. Subsequently cells were washed and sorted on a MoFlo (Dako Cytomation) cell sorter. Sorted cells were spun down, resuspended in Matrigel and grown into organoids according to standard human liver organoid culture procedure (see Human liver organoid culture). After 14 days in culture the number of organoids larger than 100 μm in diameter was scored.

Hepatocyte Percoll purification and Cyp3a4 measurement

Human hepatocyte suspensions (see Isolation of EpCAM+ cell from primary human liver) were washed as described, spun down and resuspended in 35 ml Advanced DMEM/F12 (Gibco) + 13.5 ml Percoll (GE healthcare, density 1.130 g/ml) + 1.5 ml 10x HBSS (GIBCO). Cells were pelleted at 100 g for 10 minutes and washed 3 times in Advanced DMEM/F12 (Gibco). Viable cells were counted with Trypan blue and 10.000 viable cells per 50 μl drop were seeded into matrigel. Remaining cells were stained for EpCAM as described above (see Isolation of EpCAM+ cells from primary human liver) or seeded onto collagen coated tissue culture plates for subsequent determination of cytochrome 3A4 activity. To measure Cyp3a4 in primary hepatocytes, the seeded cells were cultured in Williams E medium (Gibco) containing Hepatocyte plating supplement pack (Gibco) for 4 days with daily medium changes. On day 0 and day 4 the cells were incubated with Luciferin-PFBE substrate (50 μM) and Cytochrome P450 activity was measured using the P450-Glo Assay Kit (Promega) according to manufacturer's instructions and normalized to the number of cells in the plate. HepG2 cells cultured in the same medium served as controls.

Genetic analysis

DNA libraries for WGS analysis were generated from 1 μg of genomic DNA using standard protocols (Illumina). The libraries were sequenced with paired-end (2 x 100 bp) runs using Illumina HiSeq 2500 sequencers to a minimal depth of 30 x base coverage (average depth of ~ 36.9 x base coverage). As reference sample, liver biopsies was sequenced to equal depth for

the different donors. Sequence reads were mapped against human reference genome GRCh37 using Burrows-Wheeler Aligner (BWA) 0.7.5a with settings 'bwa mem -c 100 -M' resulting in sample-specific BAM files. To predict CNVs, BAM files were analyzed using Control-FREEC (Boeva et al., *Bioinformatics* 28, 423-5 (2012)) and DELLY (Rausch et al., *Bioinformatics* 28, i333-i339 (2012)). To obtain somatically acquired CNVs, we filtered called CNVs for occurrence in the reference samples (liver biopsies). Single nucleotide variants were multi-sampled called using the Genome Analysis Toolkit (GATK) v2.7.2 UnifiedGenotyper (DePristo et al., *Nat Genet* 43, 491-8 (2011)). We only considered positions at autosomal chromosomes, which were covered at least 20x in all liver stem cell samples and corresponding biopsy from the same donor. Candidate somatic SNVs were further filtered using the following criteria: no evidence in reference samples; minimal alternative allele frequency of 0.3 to exclude sequencing artefacts and potential substitutions that occurred after the clonal step; a minimal GATK quality score of 100; no overlap with single nucleotide polymorphisms (SNPs) in the Single Nucleotide Polymorphism Database (dbSNP 137.b37); and no overlap with SNVs in the other tested individual (Figure S2).

Immunohistochemistry, immunofluorescence and Image analysis

Tissues and organoids were fixed o/n with formalin or 4% PFA respectively, and stained washed and transferred to tissue cassettes and paraffin blocks using standard methods. Tissue sections (4 μ M) were prepared and stained with antibodies, H&E or PAS using standard techniques. The antibodies and dilutions used are listed in Table S5. Stained tissues were counterstained with Mayer's Hematoxylin. Pictures were taken with a Nikon E600 camera and a Leica DFDC500 microscope (Leica). For whole mount immunofluorescence staining, organoids were processed as described in Barker *et al.*, (Barker et al., 2010). Nuclei were stained with Hoechst33342 (Molecular Probes). Immunofluorescence images were acquired using a confocal microscope (Leica, SP5). Images were analyzed and processed using Leica LAS AF Lite software (Leica SP5 confocal). All phase contrast pictures were acquired using a Leica DMIL microscope and a DFC420C camera.

RT-PCR and qPCR analysis

RNA was extracted from organoid cultures or freshly isolated tissue using the RNeasy Mini RNA Extraction Kit (Qiagen), and reverse-transcribed using reverse-transcribed using Moloney Murine Leukemia Virus reverse transcriptase (Promega). All targets were amplified (40 cycles) using gene-specific primers and MiIQ syber green (Bio-Rad). Data were analysed using BioRad CFX manager. For Supplemental Figure S7, cDNA was amplified in a thermal cycler (GeneAmp PCR System 9700; Applied Biosystems, London, UK) as previously described (Huch et al., 2009). Primers used are listed in Table S4.

Functional hepatocyte studies

To assess glycogen storage and LDL uptake, liver organoids grown in EM or DM for 11 days were stained by Periodic acid-Schiff (PAS, Sigma) and DiI-Ac-LDL (biomedical technologies), respectively, following manufacturer's instructions. To determine albumin and A1AT secretion, liver organoids were differentiated as described. Culture medium was changed every 3-4 days and culture supernatant was collected 24h after the last medium change. HepG2 (ATCC number 77400) and HEK293T (ATCC number CRL-3216) cells were cultured for 24h in the same medium without growth factors and were used as positive and negative control respectively. The amount of albumin and A1AT in culture supernatant was determined using a human specific Albumin or human specific A1AT ELISA

kit (both from Assay Pro). To measure Cyp3a activity the cultures were differentiated as described and the day of the experiment the cells were removed from the matrigel and cultured with the Luciferin-PFBE substrate (50 μ M) in Hepatozyme medium supplemented with 10% FBS (Gibco). As controls, HepG2 and HEK293T cells were cultured for 24h in DMEM 10%FBS and the day of the experiment transferred to Hepatozyme medium supplemented with 10% FBS (Gibco) and Luciferin-PFBE substrate (50 μ M). Cytochrome P450 activity was measured 8h later using the P450-Glo Assay Kit (Promega) according to manufacturer's instructions.

Concentrations of midazolam, 1-hydroxymidazolam (1-OH-M) and 1-hydroxymidazolam-glucuronide (1-OH-MG) were determined in 50 microliter using LC-MS/MS. Analysis was carried out at the Clinical Pharmaceutical and Toxicological Laboratory of the Department of Clinical Pharmacy of the University Medical Center Utrecht, the Netherlands. All experiments were performed on a Thermo Fisher Scientific (Waltham, MA) triple quadrupole Quantum Access LC-MS/MS system with a Surveyor MS pump and a Surveyor Plus autosampler with an integrated column oven. Analytes were detected via MS/MS, with an electrospray ionization-interface in selected reaction monitoring-mode, by their parent and product ions. The method showed linearity over the range of 0.02 – 1.50 mg/L for MDZ and OHM and over the range of 0.10 – 10.0 mg/L for HMG. The analytical accuracy and precision were within the maximum tolerated bias and CV (20% for LLOQ, 15% for the other concentrations). Since a 1-OH-MG standard was not available, a Gold Standard was used. The Gold Standard consisted of the urine from two adult intensive care patients with a high dose of intravenous midazolam and good renal function. Total bile acids were measured on an AU5811 routine chemistry analyzer (Beckman Coulter, Brea, California) with an enzymatic colorimetric assay (Sentinel Diagnostics, Milano, Italy). Ammonia elimination was analysed as follows: organoid cultures were expanded and differentiated in DM medium for 8 days. On day 8 CAG was added to the medium and 3 days later the organoids were removed from the matrigel, washed with Williams' medium and subsequently incubated with 1 mL of test medium (Williams' E medium (Lonza, Basel, Switzerland) with 10% fetal bovine serum (Lonza), 5 μ g / mL insulin (Sigma, St. Louis, U.S.), 50 μ M hydrocortisone hemisuccinate (Sigma), 2mM glutamine (Lonza), 50 U / mL penicilline and 50 μ g / mL streptomycin (penicilline/streptomycine mix (Lonza), 1.5 mM NH₄Cl (Sigma), 2.27 mM D-galactose (Sigma), 2 mM L-lactate (Sigma) and 2 mM ornithine hydrochloride (Sigma)). Then 0.25 mL samples were taken after 45 min, 7 and 24 hrs and stored at -20°C for further analysis. Subsequently, all cultures were washed twice with PBS, trypsinized and cell number was counted by tripan blue exclusion.

Concentrations of ammonia were assessed in all samples by using the Ammonia (rapid) kit (Megazyme International, Wicklow, Ireland). The rates of ammonia elimination were established by calculating the changes in absolute molecular amounts of ammonia in the medium and corrected for time and cell number.

SERPINA1 sequencing

All 4 SERPINA1 exons were amplified from genomic DNA using Phusion High-fidelity DNA polymerase (Thermo Scientific) and specific primersets (see Table S4). PCR products were purified using QIAquick PCR purification kit (Qiagen) and sequenced on an ABI 3730XL capillary sequencer.

Enzymatic Elastase inhibition assay

For measurement of the inhibitory action of α 1-antitrypsin in organoid supernatants, donor and patient organoids were differentiated for 11 days. Culture medium was changed every 2-3 days and culture supernatant was collected 24h after the last medium change. For the assay, 160 μ l of supernatant are mixed with 20 μ l of a 2 mg/ml N-Succinyl-Ala-Ala-Ala-p-

nitroanilide (Sigma) 100 mM Tris pH 8.0 solution in a clear-bottom 96-well plate. After addition of 6×10^{-4} U of Elastase (porcine pancreas, Sigma) in 100 mM Tris pH 8.0, the increase in absorbance at 410 nm is measured continuously over 30 minutes. Elastase inhibition by supernatants is measured as the decreased inclination of absorbance over time in comparison to uninhibited controls (plain medium) and compared to a dilution series of purified human α 1-antitrypsin (Zemaira) in medium.

Detection of eIF2 α phosphorylation

Donor and α 1-antitrypsin deficient patient organoids were differentiated for 11 days. Culture medium was changed every 2-3 days and organoids were lysed in Lysis buffer (50 mM Tris pH 7.5, 50 mM NaCl, 0.5% Triton-X100, 0.5% NP40 substitute, 5 mM EGTA, 5 mM EDTA, 1x Complete protease inhibitor (Roche), 1x PhosStop (Roche)). Using standard techniques lysates were resolved by SDS-Page and blotted on PVDF membranes (Millipore). Antibodies against are listed in Table S5.

Supplemental References

Barker, N., Huch, M., Kujala, P., van de Wetering, M., Snippert, H.J., van Es, J.H., Sato, T., Stange, D.E., Begthel, H., van den Born, M., *et al.* (2010). Lgr5(+ve) stem cells drive self-renewal in the stomach and build long-lived gastric units in vitro. *Cell Stem Cell* 6, 25-36.

Huch, M., Gros, A., Jose, A., Gonzalez, J.R., Alemany, R., and Fillat, C. (2009). Urokinase-type plasminogen activator receptor transcriptionally controlled adenoviruses eradicate pancreatic tumors and liver metastasis in mouse models. *Neoplasia* 11, 518-528, 514 p following 528.

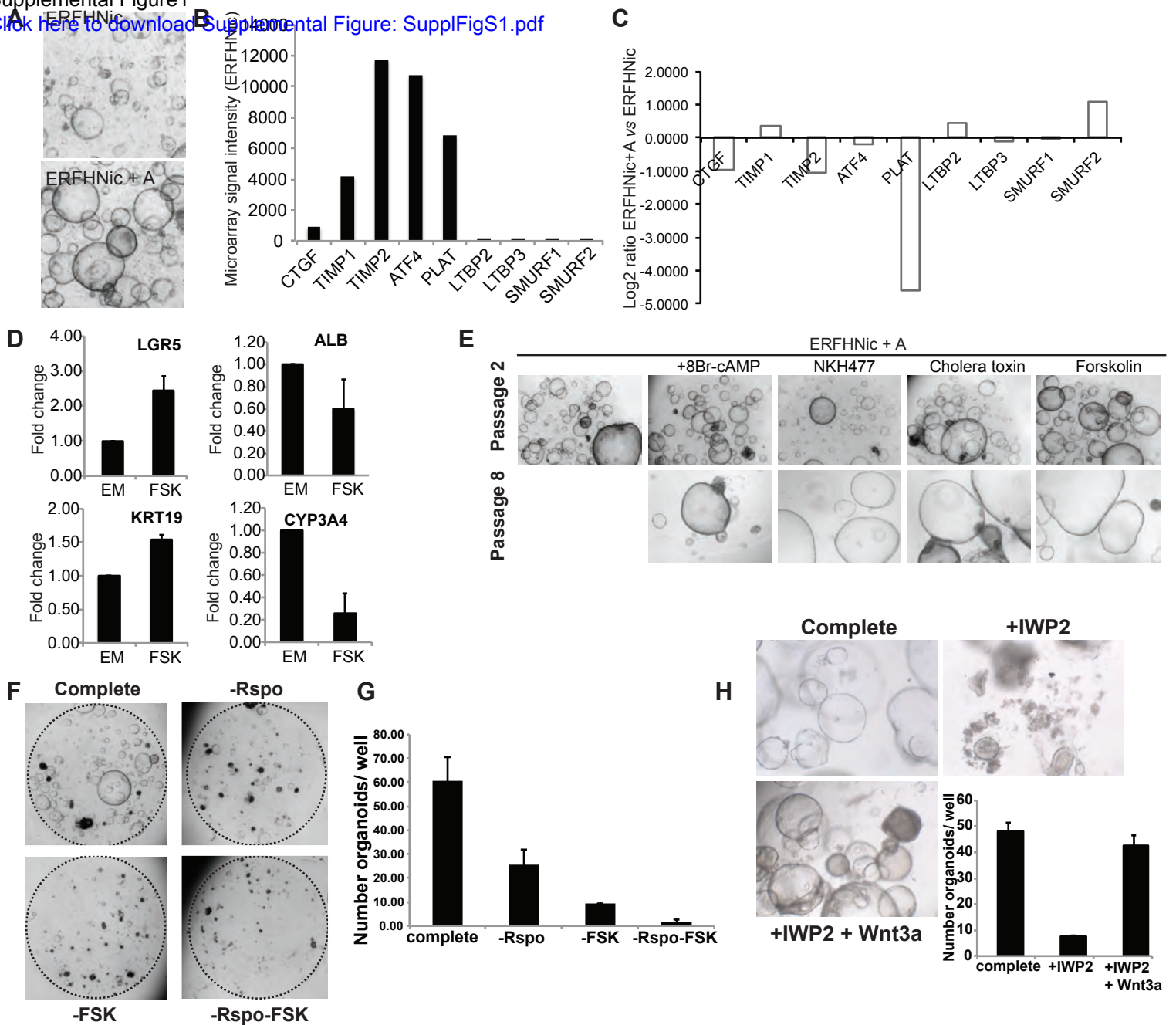


Figure S1: TgFb inhibition, active Wnt signaling and cAMP activation are essential for the long term expansion of human liver cells. Related to Figure 1.

A-E: Liver tissue was digested using collagenase dissociation as described in Material and Methods. Single cell suspensions were counted and 3000 or 10000 cells were seeded per well in a 48well plate. Cells were cultured in mouse liver medium containing Egf, Rspo, Fgf10, Hgf and Nicotinamide (ERFHNic) or the same medium supplemented with A8301 (+A) or forskolin (+FSK) or the indicated compounds. **A:** Representative images of organoid cultures grown in the mouse medium (ERFHNic) or medium supplemented with A8301 (+A). **B:** Gene expression of TGFb target genes, sequesters and inhibitors in 2 weeks old cultures maintained in mouse medium. Results are expressed as microarray signal of the specific gene after normalization. **C:** Gene expression of the specific TGFb genes downregulated upon A8301 treatment. Results are expressed as log2 fold change when comparing cultures treated vs non-treated. **D:** Gene expression of *LGR5*, *KRT19*, *ALB* and *CYP3A4* upon FSK treatment. **E:** Images of organoid cultures treated for up to 8 passages with the indicated cAMP activators. **F:** Expanding human liver organoids grown in complete medium as described in Methods were maintained in that medium (complete) or transferred to a medium without Rspo (-Rspo), without FSK (-FSK) or both (-Rspo-FSK). After withdrawal the cultures deteriorated and could not longer be passaged. Representative image of 1 donor material 7 days after withdrawal. **G:** Quantification of the number of organoids per well after a 7 days withdrawal of Rspo or FSK or both. Results are expressed as the mean \pm SEM of 2 independent human donor material and 2 independent experiments. **H:** Addition of the porcupine inhibitor (IWP2) to the medium resulted in growth arrest evident as early as 5 days after the treatment. That effect could be rescued by the exogenous addition of Wnt into the medium (+Wnt3a). Representative images taken 12 days after treatment. Organoid numbers were counted 12 days after the treatment. Graph indicating the number of organoids in the presence/absence of the indicated compounds. Results are expressed as mean \pm SEM of 2 independent human liver cultures.

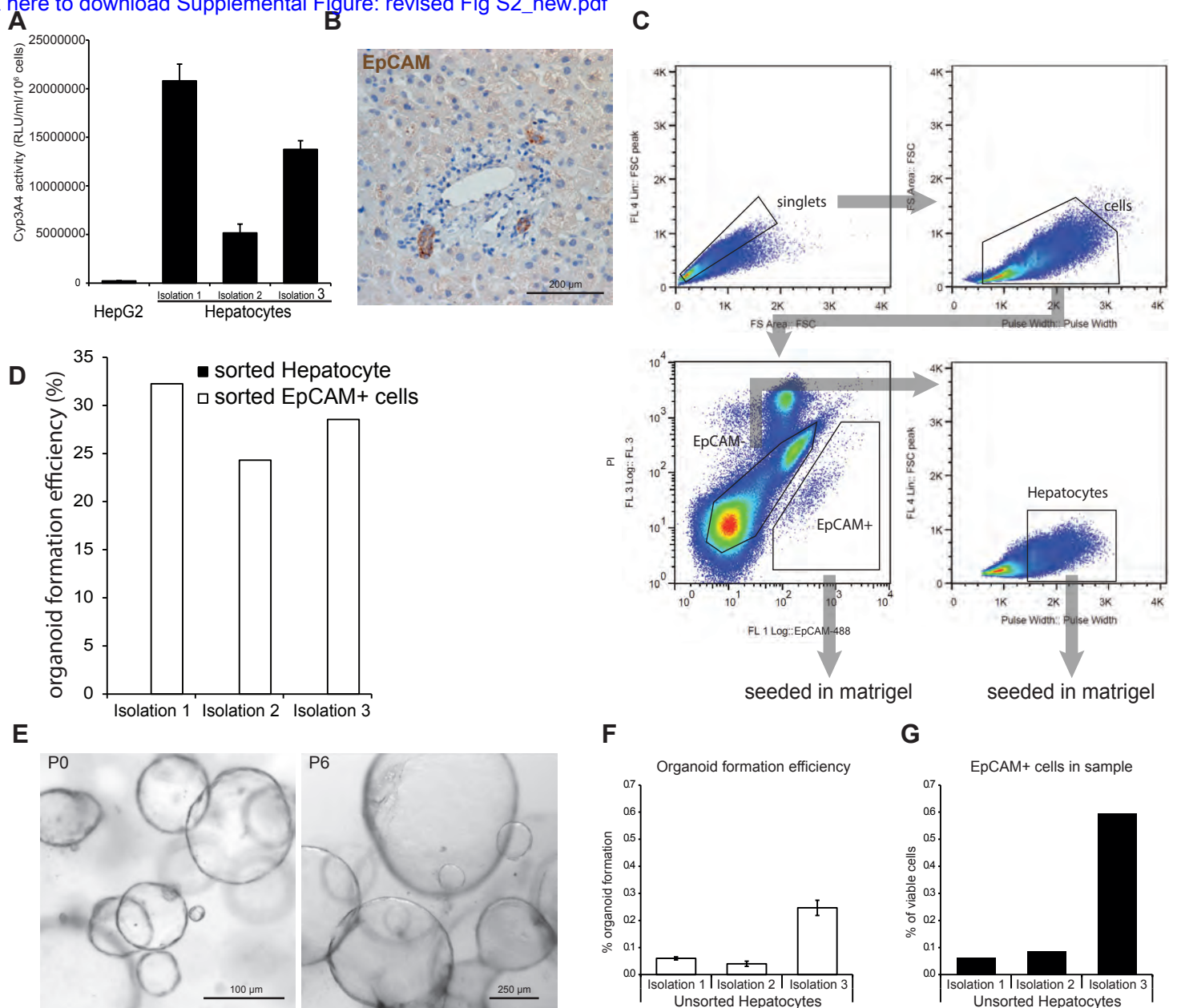


Figure S2: Human liver cultures are of ductal origin. Related to Figure 1.

(A) Cyp3A4 activity of Percoll purified primary human hepatocytes after 4 days in culture in comparison to HepG2 cells. (B) EpCAM marks bile ducts in human liver sections. Hepatocytes are EpCAM negative. (C) sorting strategy to purify EpCAM+ ductal cells and Hepatocytes. In the first step, singlets were gated to avoid contamination by cell aggregates. Subsequently, large debris and erythrocytes were excluded. From this population, EpCAM+ PI- (viable) cells were sorted as the ductal population. For hepatocyte sorting large EpCAM- cells were selected. (D) Organoid formation efficiency of sorted ductal and hepatocyte populations after 14 days. Organoids bigger than 100 μm were scored. (E) EpCAM+ sort derived organoids at passage 0 and passage 6. (F-G) Organoid formation efficiency of unsorted, Percoll purified hepatocytes (F) and the respective percentage of residual EpCAM+ cells (G).

A

FILTER STEPS	No. of base substitutions	
	Donor 1	Donor 2
1. Whole genome multi sample called	4,810,302	4,770,505
2. PASS VariantFiltration	3,847,858	3,811,373
3. >20X coverage in all samples	2,401,575	2,562,222
4. Autosomal chromosomes	2,298,543	2,524,407
5. Zero evidence in biopsy	6,520	2,548
6. PNR \geq 0.3 in subclonal culture & PNR = 0 or \geq 0.3 in other subclonal culture	2,793	1,607
7. Without dbSNP ID	2,695	1,556
8. No evidence other donor	2,691	1,555

B *Estimated base substitution False Negative Rate (FNR)*

Donor	1		2	
# Germline SNPs	2,190,637		2,426,801	
Subclonal culture	A	B	A	B
# Missed germline SNPs	66,351	66,331	62,188	62,230
FNR (%)	3.03	3.03	2.56	2.56

Figure S3: Filtering steps and FNR of all sequenced samples. Related to Figure 2

A: Total number of base substitutions after various filtering steps:

(1) Multi-sample called (biopsy, 2 parental cultures, 2 subclonal cultures for both donors) base substitutions with UnifiedGenotyper from GenomeAnalysis toolkit version 2.8-1.

(2) First quality control was performed with VariantFiltration from GenomeAnalysis toolkit version 2.8-1 with settings:

--clusterWindowSize 10

--filterExpression "MQ0 \geq 4 && ((MQ0 / (1.0 * DP)) > 0.1)" --filterName "HARD_TO_VALIDATE"

--filterExpression "QUAL < 100.0" --filterName "LowQual"

--filterExpression "QD < 1.5" --filterName "LowQD"

(3) Base substitutions with a coverage of at least 20X in all samples.

(4) Base substitutions at autosomal chromosomes.

(5) Base substitutions without any evidence in the biopsy sample (somatic events).

(6) Base substitutions were called if PNR \geq 0.3 in the subclones. Base substitutions that were called and also have evidence in the other subclone of the same individual are removed if the $0 < \text{PNR} < 0.3$ and the number of alternative reads is > 1 .

(7) Base substitutions without a dbSNP_137 identifier.

(8) Base substitutions without evidence in the other individual.

B: Estimation of False Negative Rate (FNR). The germline SNP sets consist of base substitutions that pass filter steps 1-4, are called in the biopsy of the donor with a PNR \geq 0.3 and number of alternative alleles > 1 . Subsequently, base substitutions were called in the subclonal cultures that passed filter steps 1-4 and 6. Germline SNPs that were missed in the subclonal cultures are used to calculate the FNR.

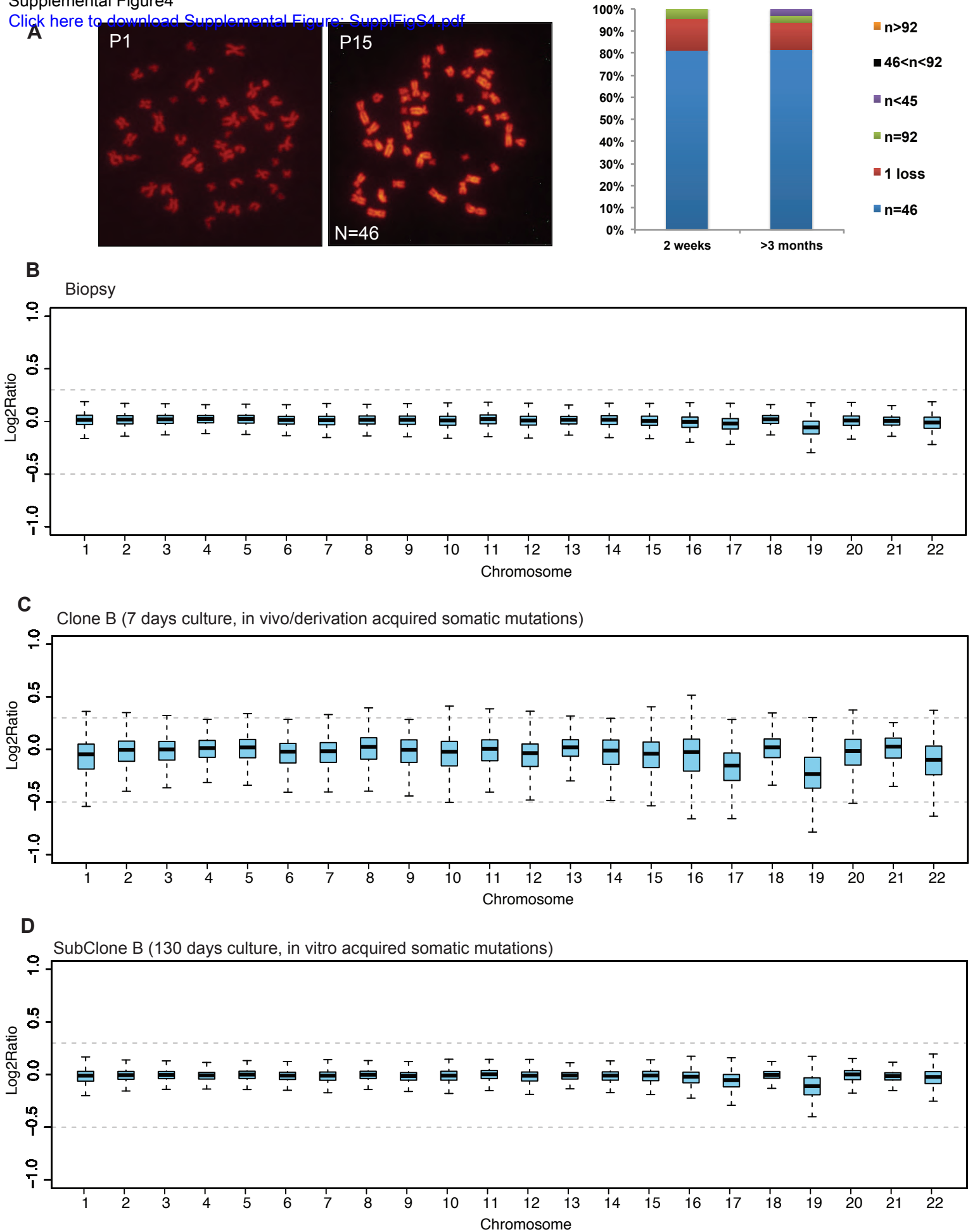


Figure S4: Genetic stability of human liver stem cell cultures. Related to Figure 3

A:Chromosome numbers were counted on a total of 76 metaphases from 2 different donors. **B-D:** Genetic stability was evaluated on clonally expanded cultures from 1 donor by WGS. Absence of DNA-Copy number alterations in human liver stem cell cultures clonally expanded long-term in culture. Box plots display the Log₂ intensity ratios for the original biopsy (**B**), clone 3 (**C**) or subclone of the clone 3 (**D**) for chromosomes 1 to 22.

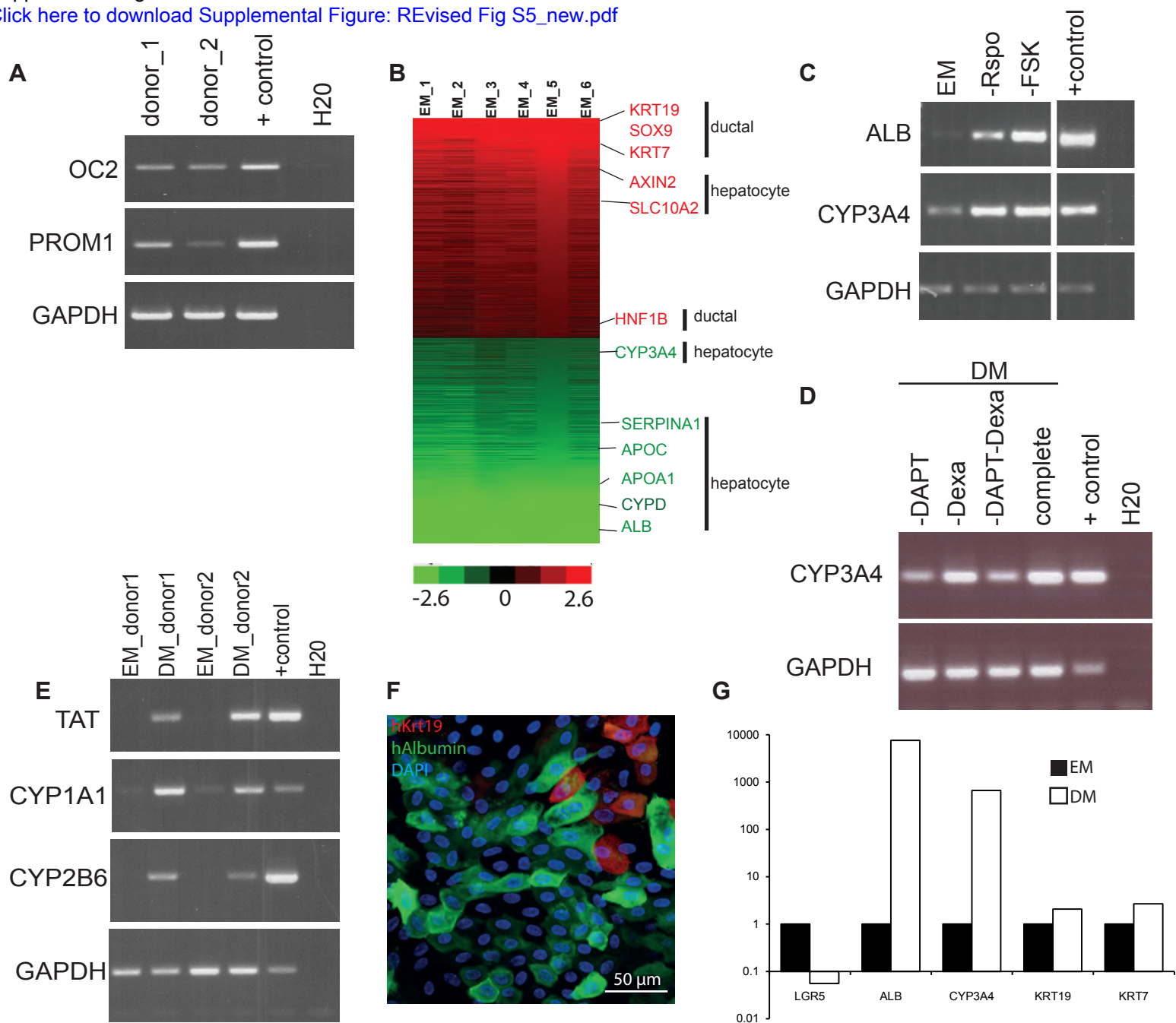


Figure S5: Analysis of organoids during expansion and upon differentiation. Related to Figure 5 and 6

(A) Representative image of RT-PCR analysis of indicated genes in 2 independent human liver donor-derived organoid cultures maintained in Expansion medium (EM) for 2 months in culture. Note expression of progenitor marker PROM1 and ductal marker OC2 (ONECUT2). **(B)** Heat map of genes >2 fold differentially expressed between human liver tissue and organoid in expansion medium. Red, upregulated. Green, downregulated, Black, not differentially expressed. **(C)** Representative image of RT-PCR analysis of indicated genes in 1 donor derived culture maintained under complete expansion medium (EM) or after withdrawal of Rspodin (Rspo) or Forskolin (FSK). **(D)** Representative image of RT-PCR analysis of CYP3A4 in 1 donor derived culture maintained under complete differentiation medium (DM, complete) for 11 days, or after withdrawal of the indicated components, DAPT and/or Dexamethasone (Dexa). **(E)** Representative image of RT-PCR analysis of indicated genes in 2 independent human liver donor derived organoid cultures maintained in Expansion medium (EM) for 2 months in culture or after 11 days in Differentiation medium (DM). Note expression of hepatocyte markers TAT and cytochromes exclusively upon differentiation. **(A-E)** + control, human liver lysate **(F-G)** EpCAM+ cell derived organoids were differentiated for 11 days according to our differentiation protocol. **(F)** Immunofluorescent Albumin and Krt19 staining show presence of differentiated cells of biliary and hepatocyte lineage. **(G)** qRT-PCR for differentiation markers of the hepatocyte (Alb and Cyp3A) and ductal (Krt19 and Krt7) lineage show successful differentiation of EpCAM+ cell derived organoids to hepatocytes.

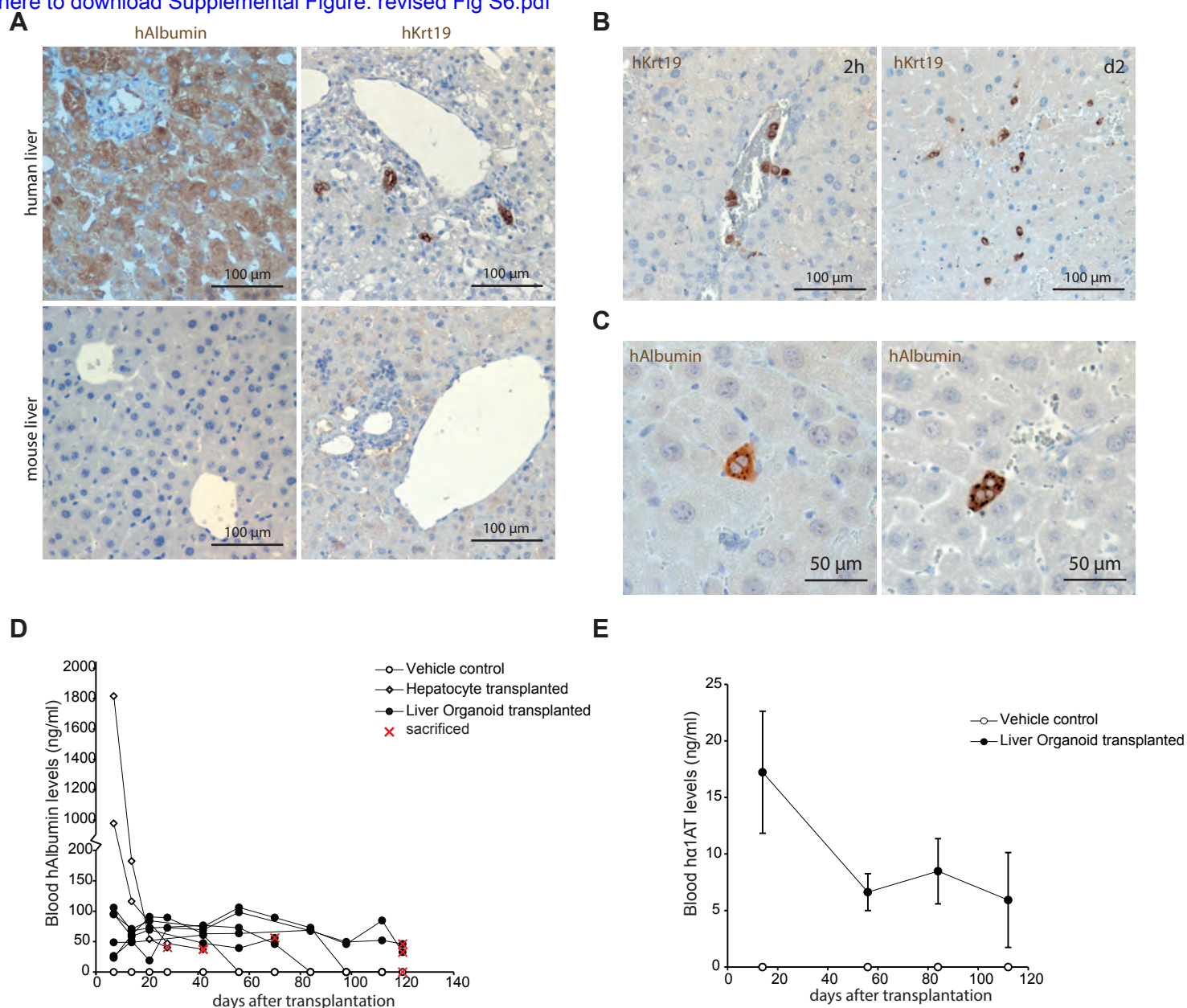


Figure S6: Transplantation of human liver organoids into damaged mouse liver. Related to Figure 6.

(A) Control staining for human specific Albumin (hAlbumin) and Kertatin-19 (hKrt19) antibodies. hAlbumin recognises human but not mouse hepatocytes, whereas hKrt19 stains human but not mouse bile ducts. (B) Liver sections of mice sacrificed 2 hours or 2 days after human liver organoid cell transplantation stained for hKrt19. After 2 hours human cells are mostly seen in blood vessels in and around portal veins, whereas cells start to engraft in the tissue 2 days after the transplant. (C) Example singlet or doublet human Albumin positive hepatocytes observed in the liver of human liver organoid transplanted Balbc/nude mice. (D) Human serum Albumin levels of individual transplanted mice over 120 days. (E) Average human serum alpha-1-antitrypsin levels of transplanted mice over 120 days. Results are shown as \pm SEM of 2 vehicle control animals and 3 human liver organoid transplanted animals.

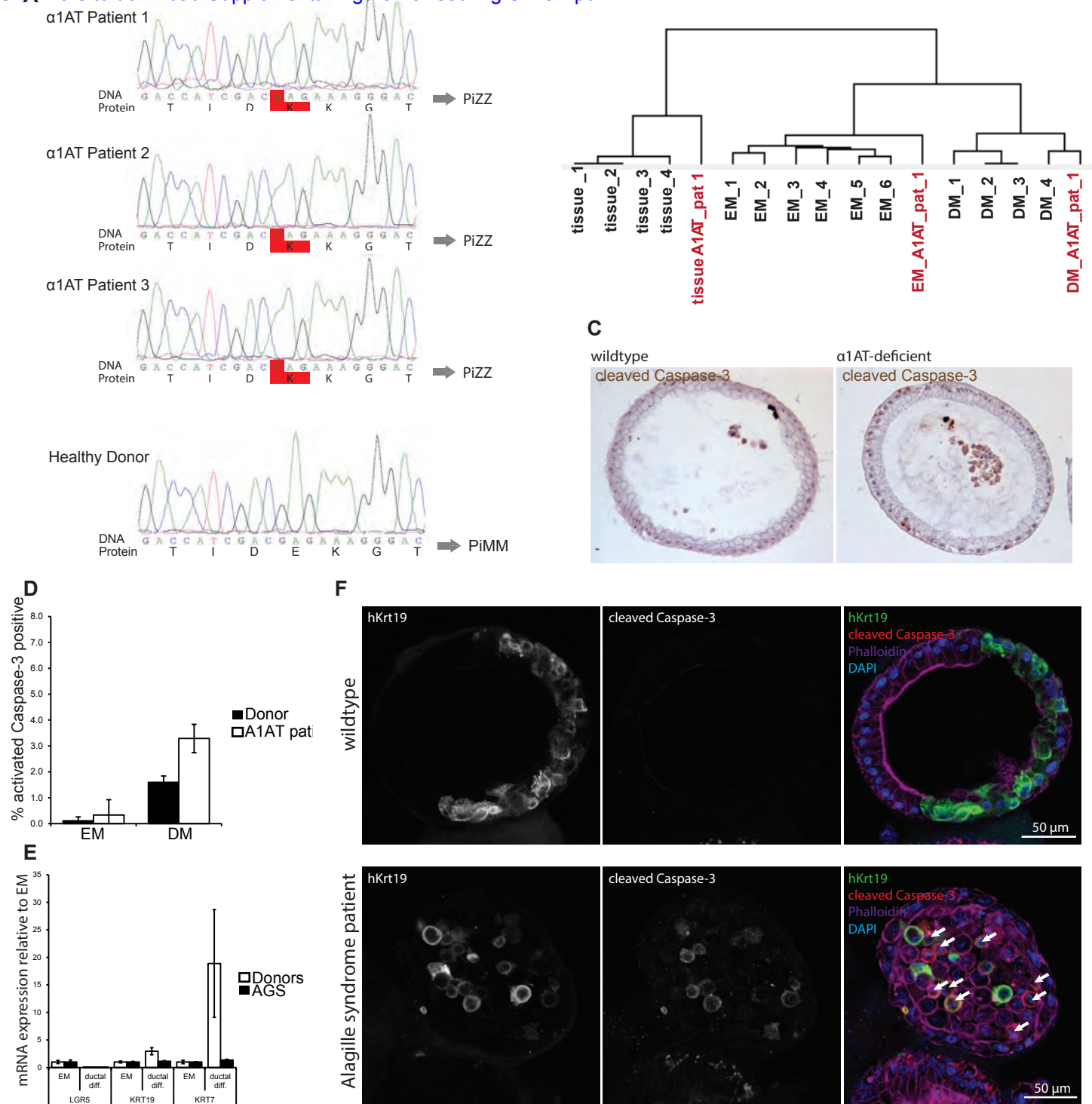


Figure S7: Organoids from A1AT-Deficiency and AGS patients mimic disease phenotypes in vitro. Related to Figure 7.

(A) SERPIN1A Sanger Sequencing of Donor #1 and α 1AT Patient #1. Chromatograms of 3 A1AT-deficient patients (PiZZ) and 1 donor with wildtype SERPINA1 (PiMM). The homozygous G to A mutation causes an amino acid change from glutamic acid to lysine at position 342. (B) Clustering analysis of the different donors (1-5) and α 1AT Patient (A1AT_pat) organoids and tissues. Note that, regarding differentiation ability, the behaviour of α 1AT Patient derived organoids resembles donor derived organoids. i.e. organoids in EM cluster cluster with donor EM organoids and α 1AT-D organoids cultured in DM cluster with donor derived organoids cultured in DM conditions. (C) histological staining for cleaved caspase-3 in donor and α 1AT Patient derived organoids differentiated in DM for 11 days. (D) quantification of apoptotic cells in wildtype and α 1AT Patient derived organoids in EM and after differentiation in DM. Results are shown as \pm SEM of 6 random sections of organoids per 2 independent donors and patients. (E) qRT-PCR of Lgr5 and ductal markers (Krt19 and Krt7) in EM and after ductal differentiation. AGS patients fail to upregulate ductal markers upon differentiation. (F) Immunofluorescence of differentiated wildtype and AGS patient organoids. Krt19 positive cells in AGS patient organoids do not integrate into the epithelium and show signs of apoptosis (arrows). EM, expansion medium. DM, differentiation medium, ductal diff, ductal differentiation medium (see text). AGS, Alagille syndrome.

Table S1: Summary of compounds tested on top of the mouse liver medium

Compound	Effect*	Function	Concentration used/tested	Source
A8301	+ keep for long term	Alk4/5/7 inhibitor	0,5µM - 5µM	Tocris 2939
Nicotinamide	+ keep for long term	PARP-1 inhibitor	10mM	Sigma N0636
AA (arachidonic acid)	+ after initiation	endogenous free fatty acid (precursor of PGE)	10µg/ml	Tocris 2756
PGE2 (prostaglandin E2)	+ after initiation but makes cystic culture	endogenous prostaglandin	10nM	Tocris 2296
Y-27632	+ after initiation	p160ROCK inhibitor	10µM	Sigma Y-27632
hES Cell Cloning & Recovery Supplement	+ after initiation	contains thiazovivin	2µM	Stemgent 01-0014-500
CHIR99021	+	GSK3b inhibitor	0,5µM	StemGent Chir99021
Wnt3a	+	Wnt agonist	30%	Conditioned Medium
BMP7	+ for differentiation	BMP agonist, Alk	25ng/ml	Peprotech 120-03
NKH 477 (forskolin analog)	+	Adenyl cyclase activator (cAMPactivator)	10µM	Tocris 1603
8-bromo-cAMP	+	cAMP analog	10µM	Tocris 1140
Cholera toxin	+	cAMP.	100ng/ml	Sigma 8052
Forskolin	+	Adenyl cyclase activator (cAMPactivator)	10µM	Tocris 1099
FGF19	+ for differentiation	FGF signaling	100ng/ml	R&D 969-FG
Jagged 1	+ mild	Notch ligand	1µM	anaspec 61298
Thiazovivin	+ after passage keep adding after passage	Rock inhibitor	2µM	Tocris 3845
SB202190	+ mild	p38 inh	300nM / 3µM	Sigma SB 202190
SB431542	+ mild	Alk5 inh	10µM	Tocris 1614
IGF	0/+ mild	Igfr ligand	100ng/ml	Peprotech 250-19
Valproic acid	0/+ mild	HDAC inhibitor	1mM	StemGent 04-0007
Byk204165	0	PARP-1 inhibitor	10µM	Tocris 3734
DR2313	0	PARP-1 PARP-2 inhibitor	40µM	Tocris 2496
Oncostatin M	0/+	Cytokine	100ng/ml	R&D 295-OM
Ciglitazone	0/+	PARP-gamma agonist	3µM	Tocris 1307
Dorsomorphin	0/+	ALK2, ALK3 and ALK6 inhibitor. AMPK inhibitor	1µM	Tocris 3093
Pyrintegrin	0/+	unknown, facilitates reprogramming(1)	10µM	Stemgent 04-0072
h noggin recombinant	0/+	BMP inhibitor/sequesters BMP	25ng/ml	Peprotech 120-10C
ID8	0/+	unknown, stimulates ESC proliferation(2)	10µM	Tocris 3853
Ascorbic acid	0/+	antioxidant	50µM	sigma 5960
Antioxidant supplement	0/+	antioxidant	1x	sigma A1345
Follistatin	0/+	Activin-binding molecule,	100ng/ml	Peprotech 120-13
FGF2	0/-	FGF signaling	10ng/ml	R&D 233-FB
DAGKi	-	Diacylglycerol kinase inhibitor	10µM	Sigma D5919
Human sRANK Ligand	-	Tnf family member, cytokine	100ng/ml	Peprotech 310-01
Zardaverine	-	PDE III/IV inhibitor.	10µM	Tocris 1046
Retinoic Acid	-	Retinoic acid signaling	10µM	Tocris 302-79-4
FBS	-	fetal bovine serum	5-50%	Gibco
human serum	-	human serum	5-50%	donated from WKZ#
IWP2	-	Porcupine inhibitor	3uM	Tocris 3533

*
positive effect to expand the cultures
mild positive effect
no effect, either positive or negative
negative effect

#WKZ= Whilhelmina KinderZiekenhuis (Utrecht)

(1)Xu, Y., et al. (2010) Revealing a core signaling regulatory mechanism for pluripotent stem cell survival and self-renewal by small molecules. Proc Natl Acad Sci USA 107: 8129-8134.

(2)Miyabayashi et al (2008) Indole derivatives sustain embryonic stem cell self-renewal in long-term culture. Biosci.Biotechnol.Biochem. 72 1242. PMID: 18460821.

Table S2: Donor and A1AT-patient material

material	gender	age	associated pathology	A1AT levels
1	M	55	donor	
2	M	74	donor	
3	F	49	donor	
4	M	14	donor	
5	M	65	donor	
6	F	51	donor	
7	F	72	donor	
8	M	53	donor	
9	M	30	donor	
10	M	34	donor	
11	M	77	donor	
12	M	43	donor	
patient 1	F	55	AAT-1	0.20 g/L
patient 2	M	64	AAT1	0.27 g/L
patient 3	M	42	AAT1	0.18 g/L

Table S4: List of primers**Primers used for gene expression analysis**

Official Gene Symbol	Official name	RefSeq Accession number	forward 5'-3'	reverse 5'-3'	PCR product (bp)	used for
ALB	Homo sapiens albumin (ALB)	NM_000477.5	CTGCCTGCCTGTTGCCAAAGC	GGCAAGTCCGCCCTGTATC	260	qPCR and RT-PCR
AXIN2	Homo sapiens axin 2 (AXIN2)	>NM_004655.3	AGCTTACATGAGTAATGGGG	AATCCATCTACACTGCTGTC	346	qPCR
BACTIN	Homo sapiens actin, beta-like 2 (ACTBL2)	>NM_001017992.3	AGTATCCTATCGAGCATGGA	CATCTTTCCCGGTTGATCT	155	qPCR
CYP1A1	Homo sapiens cytochrome P450, family 1, subfamily A, polypeptide 1 (CYP1A1)	NM_000499.3	GTGATCCAGGCTCCAAGAGTCCA	AAATCATCCGCTGCCGACC	386	RT-PCR
CYP2B6	Homo sapiens cytochrome P450, family 2, subfamily B, polypeptide 6 (CYP2B6)	>NM_000767.4	TGGCCGGGAAAAATCGCCA	GAAGAGCTAAACAGCTGGCCGAA	373	RT-PCR
CYP3A4	Homo sapiens cytochrome P450, family 3, subfamily A, polypeptide 4 (CYP3A4)	NM_017460.5	TGTGCCTGAGAACACCAGAG	GTGGTGGAAATAGTCCCGTG	226	qPCR and RT-PCR
GAPDH	Homo sapiens glyceraldehyde-3-phosphate dehydrogenase (GAPDH)	>NM_002046.4	AGAAGGCTGGGGCTATTG	AGGGCCATCCACAGTCTTC	258	RT-PCR
GAPDH	Homo sapiens glyceraldehyde-3-phosphate dehydrogenase (GAPDH)	>NM_002046.4	GCATCTTCTTTGCTCG	TGTAACCATGTAGTTGAGGT	181	qPCR
HNF4A	Homo sapiens hepatocyte nuclear factor 4, alpha (HNF4A)	NM_178850.1	CGTCTGCTCTAGGCAATGAC	ACGGACCTCCAGCAGCATCT	413	RT-PCR
HNF4A	Homo sapiens hepatocyte nuclear factor 4, alpha (HNF4A)	NM_178850.1	GTACTCTGCAGATTTAGCC	CTGTCTCATAGCTTGACCT	162	qPCR
HPRT1	Homo sapiens hypoxanthine phosphoribosyltransferase 1 (HPRT1)	>NM_000194.2	AAGAGCTATTGTAATGACCAGT	CAAAGTCTGCATTGTTTTGC	132	qPCR
KRT 19	Homo sapiens keratin 19 (KRT19)	NM_002276.4	CGCGCGTATCGGTCTCTC	AGCCTGTTCCGTCTCAAATTGGT	396	qPCR and RT-PCR
KRT7	Homo sapiens keratin 7 (KRT7)	>NM_005556.3	CTCCGGAATACCCGGAATGAG	ATCACAGAGATATTCAGGCTCC	347	RT-PCR
LGR5	Homo sapiens leucine-rich repeat containing G protein-coupled receptor 5 (LGR5)	NM_001277226.1	GACTTTAACTGAGCACAGA	AGCTTTATTAGGGATGGCAA	282	qPCR and RT-PCR
ONECUT2	Homo sapiens one cut homeobox 2 (ONECUT2)	NM_004852.2	CCCAACTCGACGCCACCA	TCTTTGGTTTTGCAGCGTCC	467	RT-PCR
PROM1	Homo sapiens Prominin 1 (PROM1, alias CD133)	NM_006017.2	ACACTGAAAGTTACATCCACAGAA	GGGTGATCCAAAACCCGGA	350	RT-PCR
RNF43	Homo sapiens ring finger protein 43 (RNF43)	>NM_017763.4	AAATTAATGAGTCCACCC	AAACTCATCAGCTTCTCAG	285	qPCR
SOX9	Homo sapiens SRY (sex determining region Y)-box 9 (SOX9)	NM_000346.3	GGAAGTCGGTGAAGAACGGG	TGTTGGAGATGACGTCGCTG	321	qPCR and RT-PCR
TAT	Homo sapiens tyrosine aminotransferase (TAT)	NM_000353.2	TGTCGCACCCGGGAGAGTT	CAAAGCACGTTGCTGGGAGGCA	238	RT-PCR

Primers used for gene sequencing analysis

Official gene symbol	Official name	RefSeq Gene	forward 5'-3'	reverse 5'-3'	PCR Product (bp)	use	Exon	mutation
SERPINA1	Homo sapiens Serpin peptidase inhibitor, clade A (alpha-1 antitrypsin, antitrypsin), member 1	NG_008290.1	ACATGTGAGCAGGAGAAACA	TTCTGGGACACTAGAGTCGTG	1228	Amplification	2	M _{Malton} , V, I
			ATCATGTGCTTACTCGGG	-	-	Sequencing		
			AGGGAGGGGACTCATGGTTT	TGCCAGTGACAAACCGTTTA	1266	Amplification	3	S, P _{Lowell} , F
			TCCAAACCTTCACTCACCCC	-	-	Sequencing		
			AAACCAAAGCCGAGTTCCCA	TTCTCGTCGATGGTCAGCAC	1158	Amplification	4	Z, M _{Wurzburg}
			GTGGTGGTCCCAGAAGAAC	-	-	Sequencing		
			TCAGCCAAAGCCCTGAGGAG	GGTGATGTCTCTCTCCC	1296	Amplification	5	Z, M _{Wurzburg} , E _{Talpa}
			TGGGATCAGCCTTACACGTG	-	-	Sequencing		

Table S5: List of Antibodies**Primary antibodies**

antigen	raised	Source and cat number	dilution	Application	fixation method & details
human Ecad	mouse	BD Biosciences (BD Transduction Laboratories™) 610182 (mouse and human)	1:500	IF	PFA 4%
human EpCAM	mouse	eBioscience, Anti-Human CD326 (EpCAM) Alexa Fluor® 488	1:100	IHC-P and FlowCytometry	Formalin + Tris-EDTA antigen retrieval
Albumin	goat	Santa Cruz ALB -N18 -sc46291	1:50 in pbs 0.1%BSA	IF	PFA 4%
human Albumin	goat	Bethyl Laboratories, Human Albumin cross-adsorbed Antibody (HRP conjugated)	1:50/1:200	IHC-P/IF	Formalin + Tris-EDTA antigen retrieval
cleaved Caspase-3	rabbit	Cell signaling, cleaved Caspase-3 #9661	1:500	IHC-P/IF	Formalin + Tris-EDTA antigen retrieval
K19	mouse	Cell Signaling #4558 -BA17	1:100 in PBS1%FBS	IHC-P/IF	Formalin + Tris-EDTA antigen retrieval
Krt7	mouse	Millipore- MAB3226	1:200	IF	PFA 4%
HNF4a	rabbit	Santa Cruz Hnf4a-(H-171) -sc8987	1:50 (not concentrated) in PBS0.1%BSA	IF	PFA 4%
ZO1	rabbit	Invitrogen ZO-1 - 40-2200	1:200 o/n 4c in PBS1% FBS	IF	Acetone fix
Mrp4	rat	Abcam Anti-MRP4 antibody [M4I-10] (ab15602)	1:20 - 1:50 in PBSO 0.03%BSA OR PBSO+1%FBS	IF	Acetone fix
EpHB2	rat IgG2A	R&D Systems EphB2 Mab (clone 512012)- MAB467	1:100,	IF	PFA
Lgr5	rabbit	Abgent LGR5/GPR49 Antibody (loop2) ID: RB14211 cat n: AP2745d LOT:SH080411H	1:100	IF and FlowCytometry	PFA
AAT1a	rabbit	Abcam Anti-alpha 1 Antitrypsin antibody - ab9373	1:500-1:1000	IHC-P	Formalin + citrate antigen retrieval
Phospho-eIF2alpha (Ser51)	rabbit	Cell Signaling # 9721	1:1000	western blot	N/A
eIF2α Antibody	rabbit	Cell Signaling #9722	1:1000	western blot	N/A
GAPDH	rabbit	Abcam-Anti-GAPDH antibody - Loading Control (ab9485)	1:2500	western blot	N/A

Secondary antibodies

antigen	raised	Source and cat number	dilution	Application
Anti-goat Alexa 488	donkey	Life Technologies- A11055 (Molecular Probes)	1:250-1:300	IF
Anti-rabbit Alexa 647	donkey	Life Technologies-A31573 (Molecular Probes)	1:250-1:300	IF
Anti-mouse Alexa 488	donkey	Life Technologies-A21202 (Molecular Probes)	1:250-1:300	IF
Anti-rat Alexa 488	donkey	Life Technologies-A-21208 (Molecular Probes)	1:250-1:300	IF
Anti mouse HRP		Dako EnVision+ System- HRP Labelled Polymer Anti-mouse	1:1-1:4	IHC-P
Anti rabbit HRP		Dako EnVision+ System- HRP Labelled Polymer Anti-Rabbit	1:1-1:3	IHC-P